1

Regional heterogeneities in the emission of airborne primary sugar compounds and biogenic secondary organic aerosols in the East Asian outflow: Evidence for coal combustion as a source of levoglucosan

M. Mozammel Haque[1,2,3], Yanlin Zhang[1,2*] Srinivas Bikkina[4], Meehye Lee[5], and Kimitaka Kawamura[3,4]

[1]*Yale-NUIST Center on Atmospheric Environment, International Joint Laboratory on Climate and Environment Change (ILCEC), Nanjing University of Information Science & Technology, Nanjing, 210044, China*
[2]*School of Applied Meteorology, Nanjing University of Information Science & Technology, Nanjing 210044, China*
[3]*Institute of Low Temperature Science, Hokkaido University, Sapporo 060-0819, Japan*
[4]*Chubu Institute for Advanced Studies, Chubu University, Kasugai 487-8501, Japan*
[5]*Department of Earth and Environmental Sciences, Korea University, Anam-dong, Sungbuk-gu, Seoul 136-701, South Korea*

Corresponding author
Yan-Lin Zhang
E-mail: dryanlinzhang@outlook.com

Atmospheric
Chemistry
and Physics
Discussions

29 **ABSTRACT**

30 Biomass burning (BB) significantly influences the chemical composition of organic aerosols

31 (OA) in the East Asian outflow. Source apportionment of BB-derived OA is an influential

32 factor for understanding their regional emissions, which is crucial for reducing uncertainties

33 in their projected climate and health-effects. We analyzed here three different classes of

34 atmospheric sugar compounds (anhydrosugars, primary sugars, and sugar alcohols) and two

35 types of biogenic secondary organic aerosol (BSOA) tracers (isoprene- and monoterpene

36 derived SOA products) in a year-long collected total suspended particulate matter (TSP) from

37 an island-based receptor site in South Korea, the Gosan. We investigate seasonal variations in

38 the source-emissions of BB-derived OA using mass concentrations of anhydrosugars and

39 radiocarbon (^{14}C-) isotopic composition of organic carbon (OC) and elemental carbon (EC) in

40 ambient aerosols. Levoglucosan (*Lev*) is the most abundant anhydrosugar, followed by

41 galactosan (*Gal*) and/or mannosan (*Man*). Strong correlations of *Lev* with *Gal* and *Man* as

42 well as their high mass ratios such as *Lev*/*Gal* (6.7±2.2) and *Lev*/*Man* (15.0±6.7), indicate the

43 contribution from hardwood burning emissions. The seasonal trends revealed that the

44 biomass-burning impact is more pronounced in winter and fall, as evidenced from the high

45 concentrations of anhydrosugars. Likewise, significant correlations were observed among

46 three primary sugars (i.e., glucose, fructose, and sucrose), emphasizing the contribution from

47 airborne pollen. The primary sugars showed higher concentrations in spring/summer than

48 winter/fall. The fungal spore tracer compounds (i.e., arabitol, mannitol, and erythritol)

49 correlated well with trehalose (i.e., a proxy for soil organic carbon), suggesting the origin

50 from airborne fungal spores and soil microbes in the East Asian outflow. These sugar

51 alcohols peaked in summer, followed by spring/fall and winter. Monoterpene-derived SOA

52 tracers were most abundant compared to isoprene-SOA tracers. Both BSOA tracers were

53 dominant in summer, followed by fall, spring, and winter. The source apportionment based

54 on multiple linear regressions, diagnostic mass ratios, and positive matrix factorization

55 analysis altogether revealed that biomass burning (41.9%) and biogenic SOA (21.1%) mostly

56 dictates the OA loading in the ambient aerosols from East Asian outflow. We also found

57 significant positive linear relationships of ^{14}C-based nonfossil- and fossil-derived organic

58 carbon fractions with *Lev-C* along with the comparable regression slopes, suggesting the

59 importance of BB and coal combustion sources in the East Asian outflow.

60

61 **Keywords:** Biomass burning tracers, primary biological aerosol particles, biogenic SOA

62 tracers, radiocarbon-based source apportionment, organic aerosols, East Asian outflow

Atmospheric
Chemistry
and Physics
Discussions

1. Introduction

Organic aerosols (OA), which account for a major fraction up to 50% of airborne total suspended particulate matter, have considerable effects on regional and global climate by absorbing or scattering sunlight (Kanakidou et al., 2005). However, the climate effects of OA are involved with large uncertainties due to our limited understanding of the contributing sources. OA can be derived from both primary emissions and secondarily formed species. Sugars are an important group of water-soluble, primarily organic compounds whose concentrations are significant in atmospheric aerosols over the continent (Jia and Fraser, 2011; Fu et al., 2008; Yttri et al., 2007; Graham et al., 2003). Anhydrosugars such as levoglucosan, galactosan, and mannosan are the key tracers of BB emissions (Simoneit, 2002). Sugar alcohols, along with glucose, trehalose and sucrose are mostly originated from primary biological particles such as fungal spores, pollen, bacteria, and viruses, and vegetative debris (Graham et al., 2003; Simoneit et al., 2004a; Bauer et al., 2008; Deguillaume et al., 2008). Primary sugars and sugar alcohols are predominantly present in the coarse mode aerosols, accounting for 0.5-10% of atmospheric aerosol carbon matter (Yttri et al., 2007; Pio et al., 2008).

Secondary organic aerosol (SOA) is a large fraction of OA, while the key factors controlling SOA formation are still poorly understood. The SOA formation significantly increased with the enhancement of the ambient aerosol mass (Liu et al., 2018). SOA is formed by both homogenous and heterogeneous reactions of volatile organic compounds (VOCs) in the atmosphere (Surratt et al., 2010; Robinson et al., 2007; Claeys et al., 2004). On a global estimation, biogenic VOCs (BVOCs) such as isoprene, monoterpenes (e.g., α/β-pinene), and sesquiterpenes (e.g., β-caryophyllene) are one order of magnitude higher than those of anthropogenic VOCs (e.g., toluene) (Guenther et al., 2006). The global emissions of annual BVOCs were estimated to be 1150 TgC/yr, accounting for 44% isoprene and 11% monoterpenes (Guenther et al., 1995). Isoprene is highly reactive and promptly reacts with oxidants such as O_3, OH, NO_x in the atmosphere to form SOA (Kroll et al., 2005, 2006; Ng et al., 2008; Surratt et al., 2010; Bikkina et al., 2021), estimated to be 19.2 TgC yr^{-1}, consisting of ~70% of the total SOA budget (Heald et al., 2008). Monoterpenes are also considered to be important sources of biogenic secondary organic aerosol (BSOA), accounting for ~35% of the global BVOCs emissions (Griffin et al., 1999).

Atmospheric aerosols in East Asia, particularly in China, are characterized by coal and biofuel combustion as a major energy source, causing vast-emission of OA into the atmosphere (Huebert et al., 2003; Zhang et al., 2016). Understanding the ambient levels OA

97   in the East Asian outflow is crucial for assessing their regional climatic effects. As part of
98   this effort, Korean Climate Observatory at Gosan (KCOG), a super site located in South
99   Korea has been chosen for investigating the atmospheric outflow characteristics from East
100   Asia (Fu et al., 2010a; Kundu et al., 2010; Ramanathan et al., 2007; Kawamura et al., 2004;
101   Arimoto et al., 1996). For instance, primary OA associated with soil/desert dust in East Asia
102   along with forest fires in Siberia/northeastern China are transported over Gosan in the spring
103   season (Wang et al., 2009a). BSOA during long-range transport from the continent and open
104   ocean, as well as local vegetation, can significantly contribute to Gosan aerosols. Although
105   these investigations were carried out almost a decade ago, no such observations are available
106   in contemporary times from Gosan. Here, we attempt to understand the current states of East
107   Asian OA using both molecular marker approach and radiocarbon data of carbonaceous
108   components.

109   The site of KCOG, located on the western side of Jeju Island adjacent to the Yellow
110   Sea and the East China Sea, is facing the Asian continent but is isolated from public areas of
111   the island (Kawamura et al., 2004). Simoneit et al., (2004b) have documented during the
112   ACE-Asia campaign that OA from the BB, and fossil fuel combustion sources are transported
113   along with desert dust to KCOG during continental outflow. An intensive campaign was
114   organized at the KCOG during spring 2005 to observe the physical properties of East Asian
115   aerosols while two dust events were detected (Nakajima et al., 2007). Here, we focus on the
116   characterization of airborne anhydrosugars, primary sugars, sugar alcohols, and BSOA
117   tracers from the KCOG. Gosan is influenced by the continental outflow from East Asia
118   during winter, spring and fall, whereas the site is influenced by the maritime air masses from
119   the Pacific Ocean and other marginal seas. This makes KCOG ideal for characterizing the
120   regional heterogeneities in the emissions of organic compounds in the East Asian outflow
121   based on the TSP samples collected during April 2013-April 2014.

122   **2. Methods**

123   **2.1. Aerosol Sampling and Prevailing Meteorology**

124   Total suspended particles (TSP) were collected on pre-combusted (450°C for 6 h) quartz fiber
125   filters (20 cm × 25 cm, Pallflex) at the KCOG (33.17 °N, 126.10 °E, see Figure 1), South
126   Korea. To get enough signal for the radiocarbon measurements, each TSP sample was
127   collected for 10–14 days from April 2013 to April 2014. A total of twenty-one samples were
128   collected using a high-volume air sampler (Kimoto AS-810, ~65 m^3 h^{-1}) installed on the
129   rooftop of a trailer house (∼3 m above the ground). After the collection, aerosol filters were
130   transferred to a pre-combusted (450°C for 6 h) glass jar (150 mL) equipped with a Teflon-

5

131   lined screw cap and transported to the laboratory in Sapporo. These TSP samples were stored

132   in a dark freezer room at -20°C until the analysis. Three field blank filters were also collected

133   during the campaign.

134   The ambient temperatures at the Gosan site were on average 6.9°C in winter, 14.1°C

135   in spring, 27.0°C in summer, and 17.1°C in fall. Likewise, the average relative humidity was

136   found to be highest in summer (71.3%), followed by spring (64.9%), fall (63.5%), and winter

137   (54.7%). Gosan is influenced by the pollution sources in East Asia during winter as well as

138   other transition periods (spring and fall) due to the prevailing westerlies. In contrast, winds in

139   summer blew mostly from the western North Pacific (WNP) by the easterly winds. The

140   spring season is, in particular, important for the transport of mineral dust mixed with polluted

141   OA to Gosan (Kundu et al., 2010).

142

143

144

145
146
147
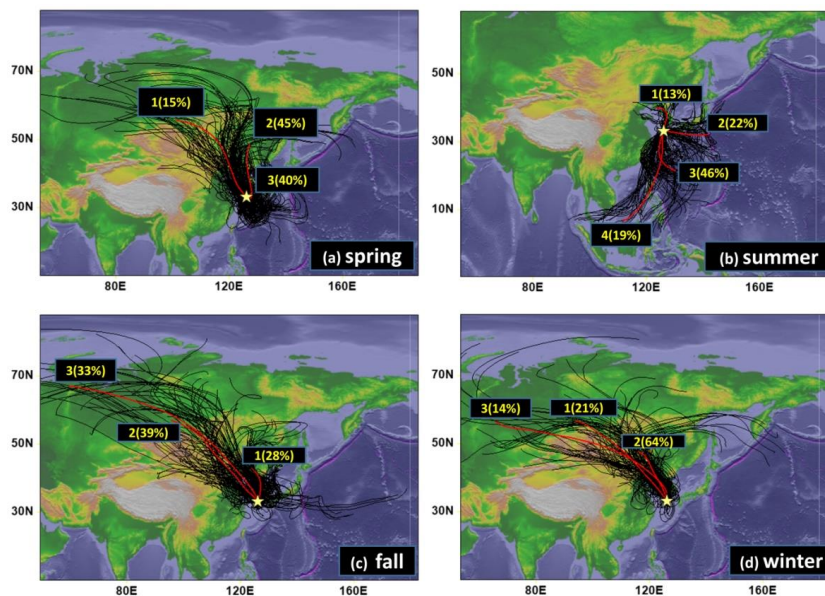148
149

150
151
152
153
154
155

156   **Figure 1.** Cluster analysis of backward air mass trajectories over Gosan (indicated by a star

157   symbol) for the TSP collected during (a) spring, (b) summer, (c) fall, and (d) winter seasons.

158

159

2.2. Extraction and Analysis of Organic Compounds

Approximately 3.14 cm^2 filter cuts were extracted with dichloromethane/methanol (2:1; v/v). The extracts were concentrated using a rotary evaporator under vacuum and then blown down to near dryness with pure nitrogen gas. The dried residues were subsequently reacted with N, O-bis(trimethylsilyl)trifluoroacetamide containing 1% trimethylchlorosilane (BSTFA+1% TMCS, SUPELCO©, Sigmaaldrich®) and pyridine at 70 °C for 3 h to derive OH and COOH groups of polar organic compounds to trimethylsilyl ethers and esters, respectively. After the derivatization followed by addition of a known amount of internal standard solution (Tridecane; 1.43 ng L^{-1} in n-hexane), the derivatized extracts were injected on to a gas chromatograph (Hewlett-Packard model 6890 GC) coupled to a mass spectrometer (Hewlett-Packard model 5973, MSD) (GC-MS). More details on the quantification of polar organic compounds using GC-MS are described in Haque et al. (2019).

The target compounds (anhydrosugars, primary sugars, sugar alcohols, and BSOA tracers) were separated on a DB-5MS fused silica capillary column (30 m x 0.25 mm i.d., 0.5 μm film thickness) using helium as a carrier gas at a flow rate of 1.0 ml min^{-1}. The GC oven temperature was programmed from 50°C for 2 min and then increased from 50 to 120°C at 30°C min^{-1} and to 300°C at 6°C min^{-1} with a final isotherm hold at 300°C for 16 min. The sample was injected in a splitless mode with the injector temperature at 280°C. The MS was operated at 70 eV and scanned from 50 to 650 Da on an electron impact (EI) mode. Mass spectral data were acquired and processed using the Chemstation software. The organic compounds were identified individually by comparison with retention times and mass spectra of authentic standards and NIST library and literature data of mass fragmentation patterns (Medeiros and Simoneit, 2007). For assessing the recoveries, ~100-200 ng of the standard solution was spiked on the blank filter and analyzed as a real sample. Overall, the average recoveries were found to be 80-104% for target compounds. The field and laboratory blank filters (n = 3) were also analyzed by the same procedures as a real sample. Target compounds were not found in the field blanks. The analytical errors based on concentrations by replicate sample analyses (n = 3) were less than 15%.

2.3. Radiocarbon isotopic composition of TC and EC

The concentrations of total carbon (TC) in TSP samples were analyzed using an elemental analyzer. For the radiocarbon isotopic composition ($\Delta^{14}C$), the aerosol filter punches were exposed for ~12 h to HCl fumes in a vacuum desiccator. Subsequently, these filters were analyzed for $\Delta^{14}C$ on a modified elemental analyzer coupled via a gas interface to Accelerator

Atmospheric
Chemistry
and Physics
Discussions

193 Mass Spectrometer Mini Carbon Dating System (MICADAS) at the University of Bern,

194 Switzerland (Salazar et al., 2015). The evolved CO_2 of TC from the elemental analyzer was

195 passed through a moisture trap (Sicapent, Merck) and isolated it from other residual gasses

196 using a temperature-controlled zeolite trap. The purified CO_2 was introduced through a gas

197 interface system to MICADAS, where $^{14}C/^{12}C$ ratios are measured according to the analytical

198 procedures detailed in Zhang et al. (2016). Likewise, the evolved CO_2 of elemental carbon

199 from the Sunset Lab OC/EC analyzer using Swiss 4S protocol (Zhang et al., 2012), was

200 directed to the MICDAS and measured for the $^{14}C/^{12}C$ ratio relative to standard calibration

201 gas. These results were expressed as fractions of modern carbon (f_M) by normalizing with a

202 $\delta^{13}C$ value of the reference standard in the year 1950 (-25‰) according to Stuiver and Polach

203 (1997) for the fractionation effects. The f_M(OC) can be estimated by using the f_M(TC) and

204 f_M(EC) in an isotope mass balance equation (Zhang et al., 2015). Additionally, we estimated

205 the relative contributions of OC and EC from the nonfossil and fossil sources ($f_{nonfossil}$ and

206 f_{fossil}, respectively) using the following equations.

207 $\quad\quad f_{nonfossil-OC} = f_M(\text{OC-sample})/f_M(\text{OC-ref}); f_M(\text{OC-ref}) \approx 1.07\pm0.04$ (1)

208 $\quad\quad f_{nonfossil-EC} = f_M(\text{EC-sample})/f_M(\text{EC-ref}); f_M(\text{EC-ref}) \approx 1.10\pm0.05$ (2)

209 $\quad\quad f_{fossil-OC} = 1 - f_{nonfossil-OC}$ (3)

210 $\quad\quad f_{fossil-EC} = 1 - f_{nonfossil-EC}$ (4)

211 $\quad\quad$ The reference values of OC and EC were obtained from Mohn et al. (2008). Using

212 the fractions of $f_{fossil-OC}$ and $f_{nonfossil-OC}$, we can, therefore, estimate the mass concentration of

213 ambient organic carbon (OC-ambient) from fossil and nonfossil sources (OC_{fossil} and

214 $OC_{nonfossil}$, respectively).

215 $\quad\quad OC_{nonfossil} = f_{nonfossil-OC} \times [OC]_{ambient}$ (5)

216 $\quad\quad OC_{fossil} = f_{fossil-OC} \times [OC]_{ambient}$ (6)

217 $\quad\quad$ More details on the radiocarbon isotopic composition data over Gosan were reported

218 elsewhere (Zhang et al., 2016).

3. Results and discussion

3.1. Trajectory/Cluster Analysis

221 Backward air mass trajectories are useful for assessing the impact of local versus regional

222 source-emissions over Gosan. Seven-day isentropic backward air mass trajectories were

223 computed using the hybrid single-particle lagrangian integrated trajectory model (HYSPLIT,

224 version 4: Stein et al., 2015) over KCOG for the sampling period using the meteorological

8

225 datasets of Global Data Assimilation System (GDAS) network. The trajectory endpoint files

226 from the HYSPLIT model were used for the cluster analysis using the Trajstat package

227 (Wang et al., 2009b) for all four seasons (Figure 1). Although cluster analysis revealed the

228 predominance of continental transport in spring, fall, and winter seasons, the air masses over

229 KCOG in summer mostly originated from the WNP. Since spring is a transition of winds

230 switching from westerlies to easterlies, Gosan is likely influenced by the long-range transport

231 of dust, pollution, and sea-salt aerosols.

232   The vertical mixing of pollutants in the boundary layer height also plays an

233 important role in controlling the strength of continental outflow along with regional

234 meteorology. For instance, the mixing height of air parcels computed by the HYSPLIT model

235 is mostly confined within 1000 m in winter but somewhat increases towards spring and fall

236 seasons (Figure S1). This vertical enhancement in the boundary layer height facilitates the

237 transport of mineral dust particles from the arid and semiarid regions in East Asia along with

238 urban pollutants to Gosan in spring and fall compared to winter. However, the strength of

239 continental outflow is somewhat dependent on several factors, including source-emissions,

240 meteorology, and mixing height of air parcels.

241   Gosan is influenced by three types of air masses in spring (Figure 1a), from

242 Mongolian Desert (cluster 1: 15%), North China (cluster 2: 45%), and the Yellow Sea

243 (cluster 3: 40%). In contrast, prevailing easterlies from the WNP mostly influence the

244 composition of TSP in summer. The cluster analysis for summer samples (Figure 1b) showed

245 four regimes, including transport from the Sea of Japan (cluster 1: 13%), WNP (cluster 2:

246 22%), South China Sea (cluster 3: 46%), and East China Sea (cluster 4: 19%). In contrast,

247 cluster analysis revealed three major transport regimes from East Asia in fall and winter

248 (Figure 1c-d). However, there exist subtle differences between winter and fall in terms of

249 influence from nearby versus distant pollution sources. For instance, long-range transport of

250 air masses from west Mongolia (cluster 1: 21%) and Russian Far East (cluster 3: 14%)

251 weakly influence Gosan in winter. Besides, we observed somewhat a larger impact of air

252 masses from the North China Plain over Gosan (cluster 2: 64%) in winter. In contrast, Gosan

253 is less influenced by air masses originating from the North China Plain, contributing ~28%

254 (cluster 1) than those from Mongolia (cluster 2: 39%) and Russian Far East (cluster 3: 33%)

255 in fall. Therefore, the impact of East Asian outflow is stronger in winter than in spring and

256 fall.

257

258

9
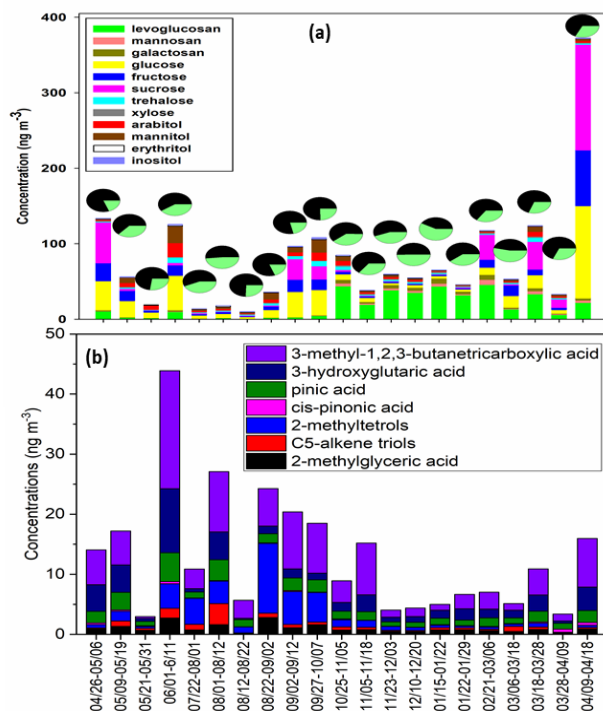
Figure 2. (a) Cumulative concentration levels of anhydrosugars, primary sugars, and sugar
alcohols (i.e., represented by bars), and depicting the contributions of nonfossil (green color)
and fossil (black color) organic carbon (i.e., pie charts), (b) Cumulative concentration levels
of isoprene- and monoterpene SOA tracers in each TSP sample collected over Gosan.

3.2. Temporal and Seasonal Variability of sugars

The temporal/seasonal trends of sugar compounds over KCOG provide useful information on
the emission strengths of various sources in the East Asian outflow. All three anhydrosugars
showed similar temporal and seasonal trends with higher concentrations in winter and fall
than spring and summer (Figure 2a). As levoglucosan and two other anhydrosugars
(mannosan and galactosan) mostly originate from the pyrolysis of cellulose/hemicellulose,
their higher loading along with more nonfossil fraction of OC (Figure 2a; pie charts) in
winter and fall indicate the impact of BB emissions. The MODIS satellite-based fire counts
(Figure S1) together with cluster analysis in winter and fall (Figure 1) have revealed an
influence of active BB emissions in the North China Plain, Mongolia and Russian Far East.
The temporal trends of glucose, fructose, and sucrose exhibited less variability throughout the
sampling period; however, a slight increase in their concentration was observed in

277 spring/summertime TSP samples (Figure 2a). Glucose and fructose have origins from leaf

278 fragments and pollen species (Fu et al., 2012a). Sucrose is a potential tracer for airborne

279 pollen (Fu et al., 2012a) and late spring/early summer is often regarded as a season for

280 "pollen-allergies". Therefore, similar temporal trends of glucose and fructose with sucrose

281 indicate their common source, pollens (Figure 2a).

282 BB also contributes to xylose and, hence, the temporal variability of xylose is

283 mimicking that of anhydrosugars. Trehalose is a primary sugar and can be used as a tracer for

284 organic carbon associated with soil dust particles (Fu et al., 2012a). Besides, the temporal

285 variability of trehalose closely resembled that of fungal spore tracers (arabitol, mannitol, and

286 erythritol), showing high concentrations in spring, summer, and fall seasons (Figure 2a) (Zhu

287 et al., 2015a; Fu et al., 2012a). KCOG is influenced by the large scale of advection of mineral

288 dust from East Asia to the WNP during these three seasons (Tyagi et al., 2017; Huebert et al.,

289 2003). The impact of mineral dust in the East Asian outflow can be traced by the high

290 concentrations of non-sea-salt Ca^{2+} in the TSP samples from Gosan (Arimoto et al., 1996).

291 Similar temporal trends of trehalose and nss-Ca^{2+}, particularly in spring samples (Figure S2),

292 suggest that the origin of fungal spores over Gosan is associated with the impact of Kosa

293 (Asian dust) events. The temporal variability of inositol is different from other sugar alcohols

294 (Figure 2a).

295 The seasonally averaged concentrations of all the anhydrosugars and xylose are

296 somewhat higher in winter/fall than spring/summer (Figure 3a-d), possibly due to a greater

297 influence of long-range transport from East Asia. In contrast, glucose, fructose, and sucrose

298 peaked in spring but decreased in other seasons (Figure 3e-g), mainly due to the contribution

299 of airborne pollen. Trehalose showed higher concentrations in fall and summer, followed by

300 spring and winter (Figure 3h). Arabitol, mannitol, and erythritol showed higher

301 concentrations in summer/fall than winter and spring (Figure 3i-k). This seasonal trend is

302 consistent with those of soil-derived fungal spores. This feature was also observed in aerosols

303 collected from the oceanic island (Okinawa) in the WNP during the impact of East Asian

304 outflow (Zhu et al., 2015a). The seasonally averaged mass concentrations of inositol are

305 highest in spring, followed by summer, fall and winter (Figure 3l). Overall, the molecular

306 compositions of anhydrosugars are characterized by the predominance of levoglucosan

307 followed by galactosan and mannosan (Figure S3). Although the temporal variability of

308 primary sugars in the TSP samples from Gosan showed a characteristic peak of glucose

309 and/or sucrose (Figure 2a), the seasonally averaged distributions are somewhat different

11

310   (Figure S3). The molecular distributions of sugar alcohols are characterized by high loadings

311   of arabitol and mannitol, followed by erythritol and inositol (Figure S3).

312
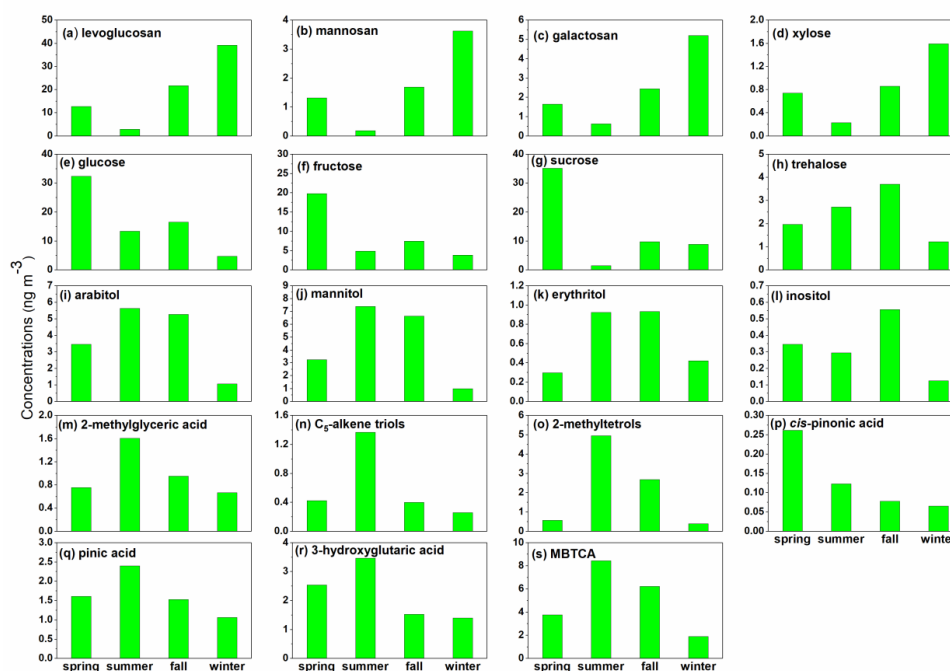
Figure 3. Seasonal variability of atmospheric levels of sugar compounds and BSOA tracers
in TSP samples from Gosan during April 2013-April 2014.

316

3.3. Temporal and Seasonal Variability of BSOA tracers

318   Six isoprene-SOA tracers such as 2-methylglyceric acid (2-MGA), three C_5-alkene triols, and

319   two 2-methyltetrols (2-methylthreitol and 2-methylerythritol) (2-MTs) were identified in

320   Gosan aerosol samples (Table 1). The sum of isoprene-SOA tracers ranged from 0.35 to 15.1

321   ng m^{-3} (avg. 3.69 ng m^{-3}) with the predominance of 2-MTs (avg. 2.09 ng m^{-3}). 2-MGA is the

322   second most abundant isoprene-SOA tracer (avg. 0.99 ng m^{-3}), a high-generation product

323   probably formed by further photooxidation of methacrolein and methacrylic acid. A similar

324   molecular composition was observed over the North Pacific and California Coast (Fu et al.,

325   2011). All the isoprene SOA tracers exhibited similar temporal variations with higher

326   concentrations in summer/spring months compared to autumn and winter (Figure 2b).

327   Conversely,   four   monoterpene-SOA   tracers,   i.e.,   *cis*-pinonic   acid,   pinic   acid,   3-

328 hydroxyglutaric acid (3-HGA), and 3-methyl-1,2,3-butanetricarboxylic acid (MBTCA), were

329 detected in Gosan samples (Table 1). Total concentrations of monoterpene-SOA tracers were

330 found to be 1.65 to 35.5 ng m^{-3} (avg. 9.24 ng m^{-3}) with a high concentration of MBTCA

331 (avg. 5.11 ng m^{-3}). All the monoterpene-SOA tracers showed similar temporal trends with

332 high values in summer/spring periods than autumn/winter (Figure 2b). Nevertheless, *cis*-

333 pinonic acid was ascribed somewhat different temporal variability with other monoterpene-

334 SOA tracers. It can be assumed that *cis*-pinonic acid might be further photo-oxidized to form

335 MBTCA (Szmigielski et al., 2007).

336   The seasonally averaged isoprene-SOA tracers were characterized with high

337 concentrations in summer, followed by spring/fall and winter (Figure 3m-o). It is of interest

338 to note that two fall samples (KOS984; 2-12 Sep and KOS986; 27 Sep to 07 Oct) exhibited a

339 high concentration of 2-MTs over Gosan (Figure 2b). We presumed that local vegetation

340 might contribute significantly to the formation of 2-MTs as it is a first-generation product.

341 Moreover, 2-MTs can be derived from the open ocean under low NO$_x$ conditions (Hu et al.,

342 2013). 3-HGA and pinic acid showed somewhat higher concentrations in summer/spring than

343 fall/winter due to the growing vegetation (Figure 3q-r). *Cis*-pinonic acid was more abundant

344 in spring compared to summer (Figure 3p) because of its photo-degradation, as discussed

345 above. In contrast, MBTCA was found to be dominant in summer/fall than spring/winter

346 (Figure 3s). The formation of MBTCA could be enhanced in fall season during atmospheric

347 transport from the East Asian continent. The molecular distributions of isoprene-SOA tracers

348 were characterized by a high loading of 2-MTs, followed by 2-MGA and C$_5$-alkene triols in

349 all seasons (Figure S3). Molecular composition of monoterpene-SOA tracers was dominated

350 by MBTCA, followed by 3-HGA, pinic acid, and *cis*-pinonic acid in all seasons (Figure S3).

351 Overall, BSOA tracers were found to be most abundant in summer, followed by fall, spring,

352 and winter (Table 1).

353   Kang et al. (2018b) reported that monoterpene-SOA tracers were more abundant than

354 isoprene-SOA tracers in spring-summer over the East China Sea, which is consistent with this

355 study. The major fraction of isoprene and monoterpenes is emitted from terrestrial plants;

356 however, the open ocean can emit isoprene and monoterpenes significantly (Conte et al.,

357 2020; Shaw et al., 2010; Broadgate et al., 1997). Air mass back trajectory and cluster analysis

358 (Figure 1) implied that air masses mostly originated from the ocean during summer. It

359 indicates that the open ocean significantly contributed to isoprene-SOA production. However,

360 terrestrial sources from the continent also substantially enhanced the formation of BSOA. For

361 Example, one sample (KOS: 979; 1-11 June 2013) during summer showed the highest

362 loading of BSOA tracers (Figure 2b), when air masses are transported from the continent

363 (Zhang et al., 2016).

364
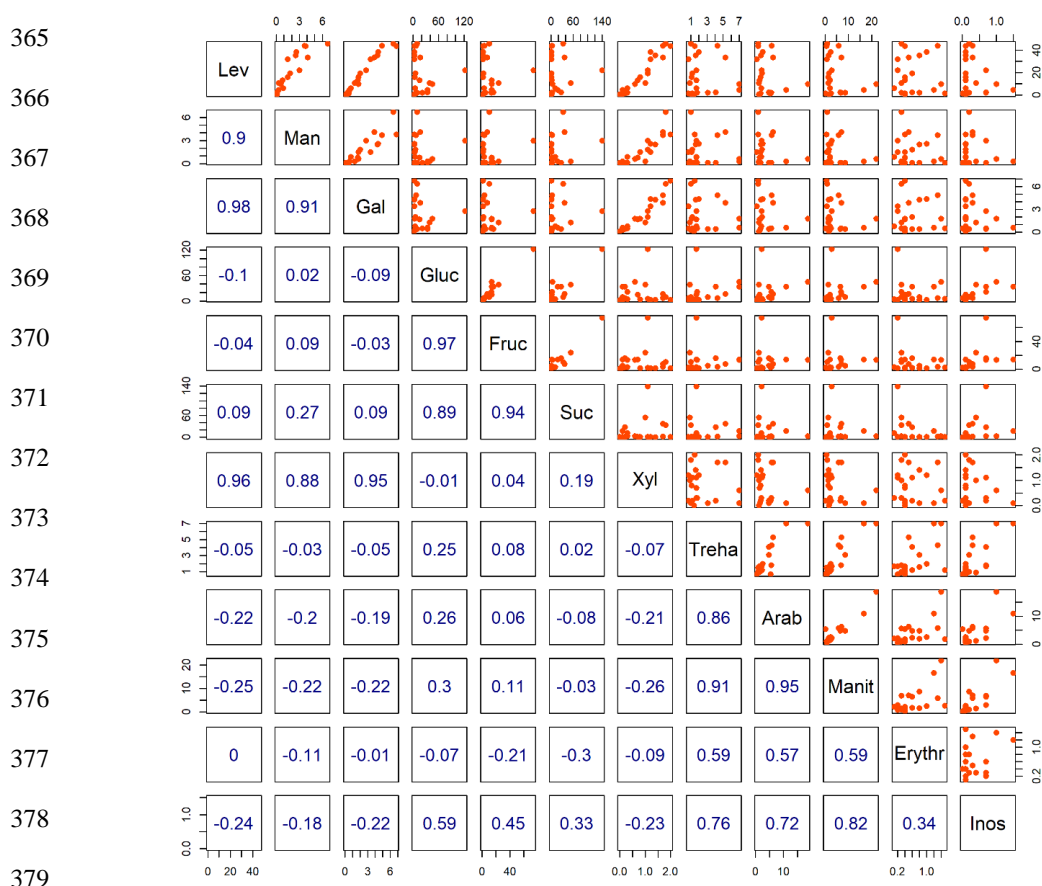
Figure 4. Multiple linear regression (MLR) analysis of airborne sugar compounds in TSP collected over Gosan.

382

3.4. Source Apportionment- Regression Analysis and Diagnostic Ratios

Anhydrosugars strongly correlated with xylose (Figure 4), suggesting their common source as BB emission in East Asia. Fu et al. (2012a) analyzed pollen from different tree species (*e.g.*, White birch, Chinese willow, Peking willow, Sugi, Hinoki), which are enriched in sucrose (182-37,300 μg g^{-1}), glucose (378-3601 μg g^{-1}) and fructose (162-1813 μg g^{-1}). In our samples, sucrose strongly correlated with glucose and fructose (Figure 4), suggesting their

Atmospheric
Chemistry
and Physics
Discussions

389   origin from plant-derived airborne pollen. Likewise, a strong correlation was found between

390   arabitol and mannitol, indicating a mutual origin from a similar type of fungal spores (Zhu et

391   al., 2015a; Fu et al., 2012a; Bauer et al., 2008; Yttri et al., 2007). Bauer et al. (2008) ascribed

392   weak correlations between arabitol and mannitol to the diverse nature of ambient fungal

393   spores. Furthermore, both sugar alcohols correlated well with trehalose, a tracer for soil

394   organic carbon (Fu et al., 2012a). This observation suggests their common origin from soil

395   organic matter associated with fungal spores. Erythritol also originates from fungal spores;

396   however, its abundance is affected by the atmospheric aging process. Kessler et al. (2010)

397   reported that erythritol is degraded during long-range transport in 12.7 days. Consequently,

398   arabitol and mannitol were moderately correlated with erythritol in the Gosan samples due to

399   the degradation of latter sugar alcohol in the East Asian outflow.

400   The linear relationship of levoglucosan (*Lev*) with mannosan (*Man*), galactosan (*Gal*),

401   and nss-K^+ provide useful information on the type of BB emissions (hardwood, softwood, or

402   crop-residue). Different types of biomass are characterized by the distinct *Lev/Man* ratios. For

403   instance, *Lev/Man* ratios from the softwood burning emissions (3-10) are different from those

404   of hardwood (15-25) and crop-residues (>40) (Singh et al., 2017; Schmidl et al., 2008a, b; Fu

405   et al., 2008; Engling et al., 2006, 2009; Fine et al., 2001, 2004). We found the *Lev/Man* ratios

406   (Table 2) over KCOG overlap between seasons and somewhat close to that of hardwood

407   burning emissions in northern China, Mongolia, and Russian Far East, as corroborated by the

408   backward air mass trajectories and MODIS fire counts (Figures 1 and S1). Besides, *Lev*/K^+

409   and *Man/Gal* ratios in summer are different from those of other seasons (Table 2). Cheng et

410   al. (2013) have apportioned qualitatively the possible source contributions of anhydrosugars

411   over a receptor site based on the comparison of *Lev*/K^+ and *Lev/Man* ratios in aerosols to

412   those from various sources profiles compiled from the literature. This approach of using the

413   mass ratios of *Lev/Man* and *Lev*/K^+ has been proven useful for deciphering the difference in

414   BB-derived OA (Bikkina et al., 2019).

415   Here, we adopted this methodology to ascertain the likely contributing sources of

416   anhydrosugars, which are BB tracers from different seasons (Figure 5). This source

417   apportionment relies on the fact that *Lev*/K^+ from the softwood burning (10-1000) is

418   somewhat higher than that of hardwood (1-100) (Fine et al., 2004). In contrast, *Lev/Man*

419   ratios for softwood are lower than those of hardwood burning (10-100) (Fine et al., 2004).

420   Likewise, *Lev*/K^+ and *Lev/Man* ratios from grasses and crop-residues are 10-100 and 0.01-

421   1.0, respectively (Bikkina et al., 2019). On a similar note, the *Lev*/K^+ ratios from the burning

422   of pine needles (0.1-1.0) somewhat overlap with hardwood burning emissions but are

Atmospheric
Chemistry
and Physics
Discussions

Open Access

EGU

423   characterized by distinct *Lev/Man* ratios (Bikkina et al., 2019). The burning of dead leaves

424   (duff) showed higher *Lev*/K^+ than that of pine needles and grasses, but their *Lev/Man* is on

425   the lower side than the former biomass type and the softwood burning emissions. However,

426   *Lev* is more susceptible to degradation during transport and, hence, the hardwood *Lev*/K^+

427   ratios could slightly shift downwards. Therefore, caution is required while interpreting the

428   ambient data from a receptor site (Bikkina et al., 2019). Overlapping the seasonal data on this

429   scatter plot of *Lev*/K^+ versus *Lev/Man* (Figure 5) clearly revealed a mixed contribution of

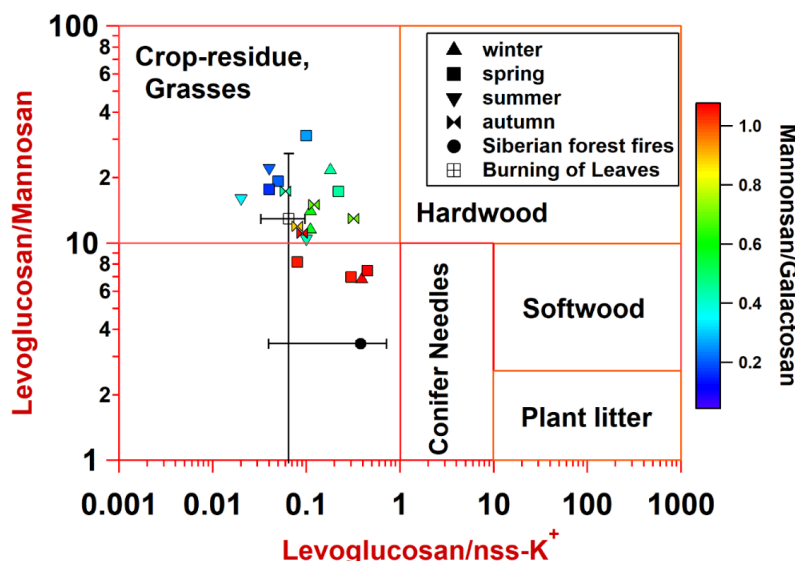430   burning of hardwood and crop-residue in the East Asian outflow.

431

432

Figure 5. Scatter plot of levoglucosan/K^+ versus levoglucosan/mannosan ratios in TSP collected over Gosan during April 2013-April 2014. The data for Siberian forest fires and burning leaves were adopted from Sullivan et al. (2008).

445

446   The correlation coefficients and diagnostic ratios of BSOA tracers specify their source

447   origin or formation pathway. 2-MGA showed significant correlation with 2-MTs (r = 0.79,

448   p<0.01) and C_5-alkene triols (r = 0.50, p<0.05) (Figure 6a-b), suggesting their similar

449   formation pathway or common sources of isoprene SOA tracers. However, a poor correlation

450   coefficient between 2-MTs and C_5-alkene triols (r = 0.33, p = 0.13) (Figure 6c) indicates their

451   different formation process over the Gosan atmosphere. Wang et al. (2005) documented that

452   polyols are formed from isoprene through diepoxy derivatives, which further convert into 2-

Atmospheric
Chemistry
and Physics
Discussions

453   MTs by acid-catalyzed hydrolysis. On the other hand, C_5-alkene triols are produced from the

454   precursor of hydroxyperoxy radicals that are initially derived from isoprene through

455   rearrangement reactions (Surratt et al., 2006). It can be noted that the formation mechanisms

456   of 2-MGA and 2-MTs are different while depending on the NO_x concentrations (Surratt et al.,

457   2010). Thus, the ratio of 2-MGA/2-MTs attributes to the influence of NO_x on isoprene SOA

458   formation. We found a low ratio of 2-MGA/2-MTs (0.67) (Figure S4a, Table 2) in summer,

459   implying enhancement of 2-MTs formation over the open ocean due to the low-NO_x

460   environment in the ocean-atmosphere. On the contrary, 2-MGA/2-MTs ratios for other

461   seasons were >1.0 (Figure S4a, Table 2), indicating an elevated formation of 2-MGA through

462   continental high NO_x condition, which is consistent with air masses back trajectory.

463
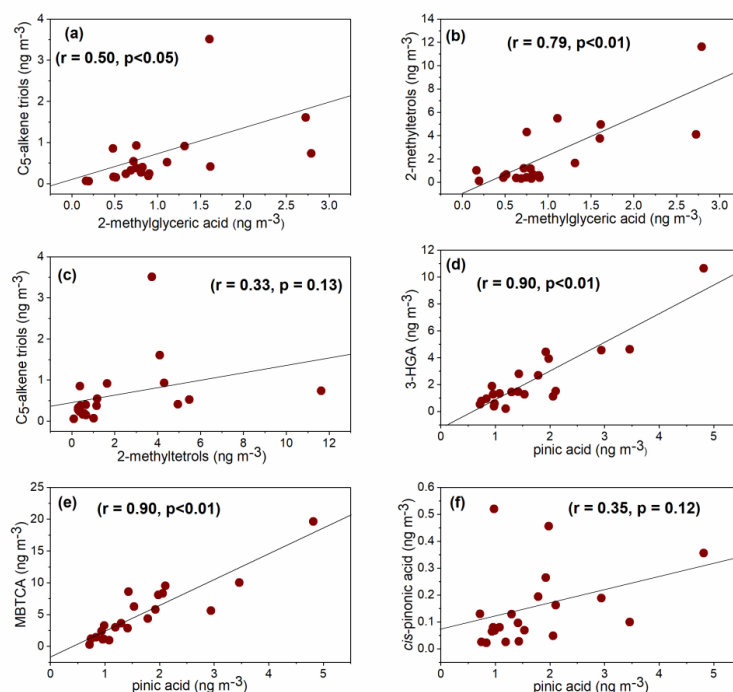
465   **Figure 6.** Pearson linear correlation coefficient analysis of BSOA tracers in Gosan TSP
466   aerosols during April 2013-April 2014.

467

468   *Cis*-pinonic acid showed poor correlation with pinic acid (r = 0.35, p = 0.12) (Figure

469   6f), suggesting that they formed from different monoterpenes such as *α*-pinene, *β*-pinene, or

470   δ-limonene. In contrast, pinic acid exhibited a strong linear correlation with 3-HGA (r = 0.90,

471   p<0.01) and MBTCA (r 0.90, p<0.01) (Figure 6d-e), implying their similar sources. It should

472   be noted that the formation processes of pinic acid, 3-HGA, and MBTCA are different

473   because pinic acid is a first-generation product, and 3-HGA and MBTCA are high-generation

474   products (Claeys et al., 2007; Müller et al., 2012; Szmigielski et al., 2007). The ratio of cis-

475   pinonic acid + pinic acid to MBTCA (P/M) is used to evaluate the aging of monoterpene

476   SOA.

477   A low P/M ratio suggests possible transformation of cis-pinonic and pinic acids to

478   MBTCA and thus relatively aged monoterpene-SOA, whereas a high ratio reflects relatively

479   fresh monoterpene-SOA (Gómez-González et al., 2012; Ding et al., 2014). Gómez-González

480   et al. (2012) reported aged monoterpene-SOA (P/M = 0.84) from a Belgian forest site while

481   fresh chamber-produced α-pinene-SOA tracers showed P/M ratios of 1.51 to 3.21 (Offenberg

482   et al., 2007). The average ratio of P/M in this study showed 0.62 with the low value in

483   summer (Figure S4b, Table 2), which is lower than those of Guangzhou (fresh monoterpene-

484   SOA; 28.9) while the air masses originated from southern China (Ding et al., 2014). It

485   indicates that monoterpene SOA in Gosan aerosol was relatively aged, particularly in summer

486   when extensive photochemical oxidation occurred due to the high temperature and intense

487   solar radiation.

3.5. Source Apportionment - Positive Matrix Factorization (PMF) Analysis

489   We used the positive matrix factorization (PMF) analysis of airborne sugar compounds and

490   BSOA tracers to assess their sources over Gosan. Five-factor profiles were chosen that could

491   best explain the data (Figure 7). In factor 1, we found higher loadings of sucrose (88%),

492   fructose (57%), and glucose (40%). Sucrose is a well-known tracer for airborne pollen as

493   these types of biogenic sources also contain significant levels of glucose and fructose; we

494   attribute this factor to contribution from "pollen". Likewise, factor 2 has higher loadings of

495   C_5-alkene triols (54%), 2-MGA (38%), cis-pinonic acid (34%), pinic acid (33%), and 3-HGA

496   (33%). These SOA tracers are formed by the photochemical oxidation of BVOCs (e.g.,

497   isoprene and monoterpene), which are emitted from terrestrial vegetation and oceanic

498   phytoplankton. Therefore, we attribute factor 2 to biogenic secondary oxidation products.

499   Factor 3 was abundantly loaded by non-sea-salt fraction of calcium (nss-Ca^{2+}), implying that

500   the component is associated with soil dust as nss-Ca^{2+} is a specific tracer of Earth surface soil

501   (Athanasopoulou et al., 2010; Brahney et al., 2013). It should be noted that significant

502   loadings were also observed for trehalose (39%), glucose (35%), and fructose (35%) in factor

503   3, indicating their association with soil microbes.

18
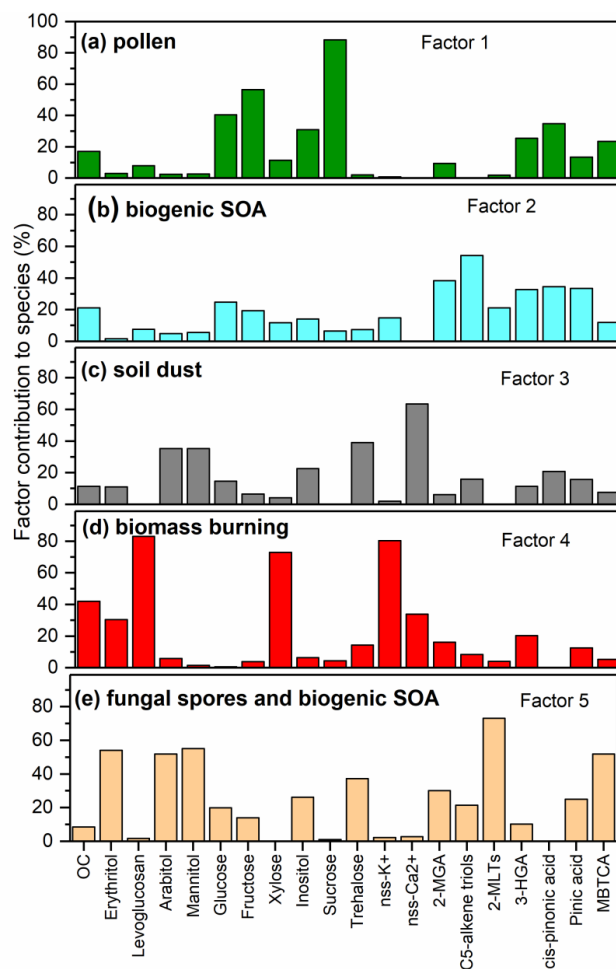
Figure 7. Positive Matrix Factorization (PMF)- based Source profiles resolved for the measured primary saccharides in TSP collected over Gosan during April 2013-April 2014.

We found higher loadings of levoglucosan (83%), nss-K$^+$ (80%), and xylose (73%) in factor 4. Large contributions were observed for the levoglucosan and K$^+$ (hemicellulose/cellulose pyrolysis tracers) and xylose (wood sugar). We, therefore, ascribe this factor to BB emissions. Factor 5 is dominated by 2-MTs (73%), MBTCA (53%), mannitol (55%), erythritol (54%), and arabitol (52%). 2-MTs and MBTCA are BSOA tracers, which are produced by the photo-oxidation of isoprene and monoterpene, respectively. In contrast, arabitol, mannitol and erythritol are typical tracers of airborne fungal spores (Lewis

516 and Smith, 1967; Bauer et al., 2008). Thus, factor 5 is associated with mixed sources of

517 'fungal spores' and 'biogenic secondary oxidation products'. PMF results were further

518 utilized to calculate the relative contributions from various sources to OC over Gosan (Figure

519 S5). BB was the dominant source of OC over Gosan (41.9%), followed by BSOA (21.1%),

520 pollen (17.1%), and soil dust (11.4%).

521 **3.6. Relative Abundances in WSOC and OC**

522 Levoglucosan is the most abundant anhydrosugar, contributing 0.05-1.54% of WSOC and

523 0.03-1.02% of OC. Likewise, sucrose, glucose, and fructose were more abundant primary

524 sugars, contributing 0.01-2.83%, 0.03-1.22%, and 0.02-0.74% of WSOC, respectively.

525 Contributions of the three primary sugars largely varied from 0.05% to 3.41% of OC.

526 Arabitol and mannitol are the most abundant sugar alcohols, whose contribution to WSOC

527 and OC ranged from 0.02% to 0.93% and 0.01% to 0.85%, respectively. Figure 8 depicts the

528 contribution of sugar compounds to WSOC and OC in TSP collected over Gosan during the

529 study period. We also compared the atmospheric abundances of sugar compounds from

530 Gosan with the literature data (Table 3). This comparison revealed the less influence of BB

531 tracer compounds (i.e., anhydrosugar levels) over Gosan, that is, a factor of 5-10 times lower

532 than those reported for the BB-influenced source regions in China and East Asia (Fu et al.,

533 2012b; Kang et al., 2018a; Wang and Kawamura, 2005; Wang et al., 2012). However, the

534 levels of anhydrosugar over Gosan are higher than those observed over the remote Canadian

535 High Arctic site (Fu et al., 2009a). In contrast, Gosan is characterized by high concentrations

536 of primary sugars compared to other remote sampling sites in Table 3. This could be

537 explained by the overwhelming contribution of primary sugars associated with soil dust

538 particles over Gosan during the East Asian outflow. Such high loadings of primary sugars

539 were observed from other remote island receptor sites in the WNP (Okinawa) during the

540 spring season (Zhu et al., 2015a). Likewise, the concentrations of sugar alcohols from Gosan

541 are somewhat similar to those from other receptor sites influenced by the East Asian outflow

542 (Verma et al., 2018; Zhu et al., 2015a).

543

544

545

546

547
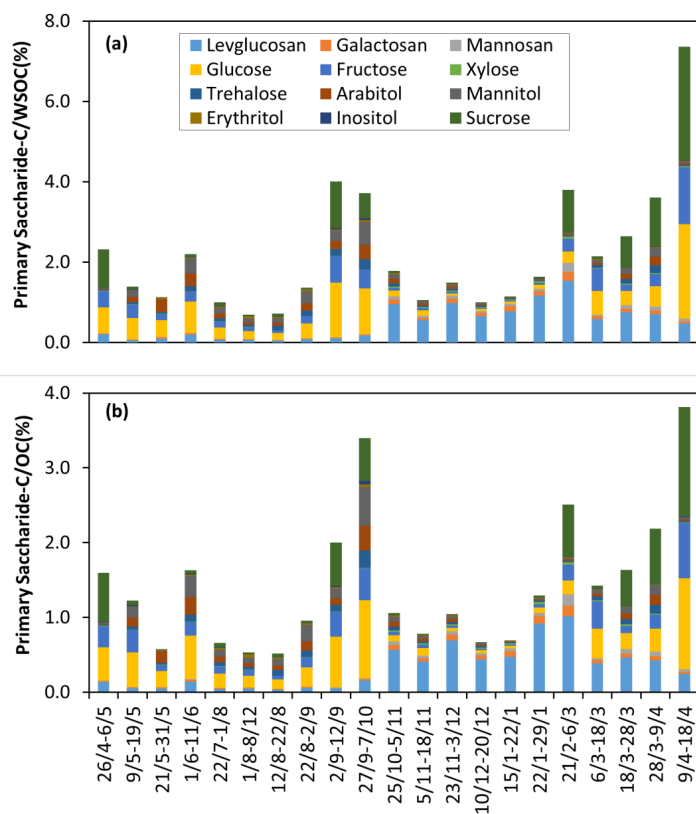
Figure 8. Contribution of primary saccharide-C in (a) WSOC(%) and (b) OC(%) in TSP collected over Gosan during April 2013-April 2014.

550

Contributions of isoprene-SOA tracers to ambient OC (0.01-0.40%, ave. 0.09%) and WSOC (0.02-0.57%, 0.13%) were lower than monoterpene-derived SOA (0.04-0.63%, 0.23% for OC and 0.06-0.82%, 0.33% for WSOC). The contributions of isoprene oxidation products to OC and WSOC were found to be highest in summer (0.23% and 0.32%, respectively), followed by fall (0.09% and 0.13%), spring (0.04% and 0.06%), and winter (0.02% and 0.03%). Likewise, the contributions of monoterpene-SOA products to aerosol OC and WSOC exhibited highest value in summer (0.40% and 0.55%, respectively), followed by fall (0.24% and 0.35%), spring (0.18% and 0.27%), and winter (0.10% and 0.14%). We found that the contribution of BSOA products to carbonaceous components was twice in summer than those of other seasons (Figure 9, Table 2). This result indicates that SOA formation was occurred in summer to a greater extent due to the intensive BVOCs emission with key factors of meteorological parameters (higher temperature and radiation).

563

564
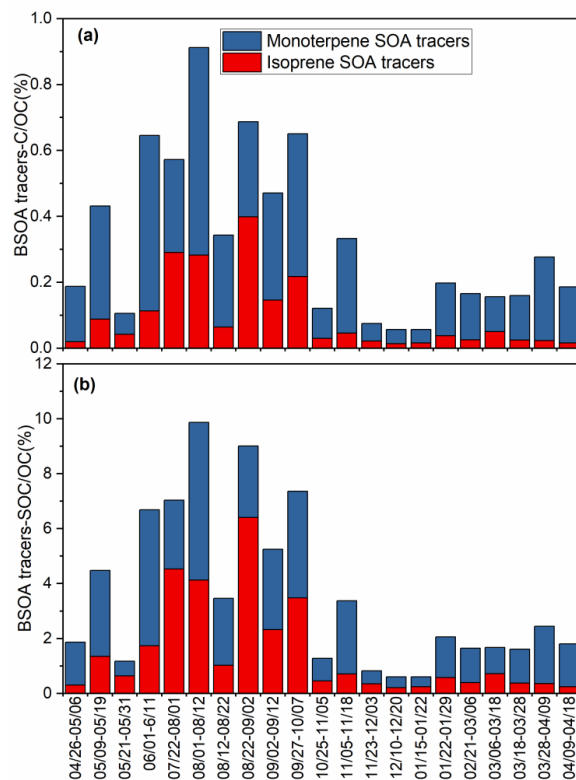
Figure 9. Contribution of (a) isoprene- and monoterpene SOA tracers-C in ambient OC(%) and (b) isoprene- and monoterpene SOA tracers-SOC in ambient OC(%) in Gosan aerosol samples during April 2013-April 2014.

568

569   We estimated secondary organic carbon (SOC) derived from isoprene and
570 monoterpenes, using the measured values of BSOA tracers and following the SOA tracer-
571 based method first proposed by Kleindienst et al. (2007). A summary of the estimated SOC is
572 provided in Table 2. The contribution of isoprene to SOC was calculated 2.26 to 97.4 ngC m^{-3}
573 (avg. 23.7 ngC m^{-3}), accounting for 1.45% of OC and 35.5% of total BSOC with the
574 predominance in summer (3.56% and 46.6% for OC and SOC, respectively). The estimation
575 of monoterpene SOA to SOC (avg. 40.1 ngC m^{-3}) was observed around two times higher than
576 isoprene (Table 2). Interestingly, the contribution of monoterpene-derived SOC to ambient
577 OC (3.65%) was dominant in summer, but monoterpene SOC to total SOC (72.1%) was most

578 abundant in spring (Figure 9b). The seasonal distributions of biogenic SOC (Table 2) implied

579 that a substantial amount of SOC was formed from monoterpenes during the spring season.

580 The estimated biogenic SOC in this study is almost one order of magnitude lower than those

581 from the continental site in south China urban area (PRD: 446 ngC m^{-3}) (Ding et al., 2012);

582 however, much higher than a remote site in the Canadian High Arctic (Alert: 9.4 ngC m^{-3})

583 (Fu et al., 2009b) and comparable with over the East China Sea (Kang et al., 2018b).

584 It should be noted that concentrations of SOA tracers cannot always provide the

585 actual contribution of the biogenic source to ambient organic aerosol mass. For example,

586 loadings of monoterpene-SOA tracers were lower in sample KOS999 (28 March - 9 April

587 2014) (3.02 ng m^{-3}) compared to sample KOS1000 (9 - 18 April 2014) (14.4 ng m^{-3}), whereas

588 estimated contribution of SOC to ambient OC showed an opposite trend (KOS999: 2.08%;

589 KOS1000: 1.56%). This result demonstrates that the estimation of SOC is an important factor

590 to evaluate the contribution of BSOA to organic aerosol mass. We calculated biogenic OC

591 using radiocarbon (^{14}C) data following the method proposed by Szidat et al. (2006). Biogenic

592 OC showed poor correlation with biogenic SOC (r = 0.36, p = 0.09) but significant linear

593 relationship with primary sugars (i.e., glucose, fructose and sucrose) (r = 0.54, p<0.5),

594 suggesting that primary bioaerosols from plant-derived airborne pollen dictate on biogenic

595 OC in Gosan aerosols.

3.7. Significance of Fossil Fuel as a source for Levoglucosan

597 The ambient levoglucosan levels showed a significant linear relationship with the OC_{fossil},

598 suggesting the fossil source contribution of this molecular marker (Figure 10a). However,

599 such a significant correlation was not evident between OC_{fossil} and other major sugar

600 compounds. Until recently, *Lev* has been thought to originate primarily from the

601 hemicellulose/cellulose pyrolysis of vegetation and, hence, can be employed as a powerful

602 tracer for biomass smoke particles (Fraser and Lakshmanan, 2000; Simoneit et al., 1999).

603 Residential coals (*e.g.,* lignite and bituminous coal) have been shown to contain high

604 concentrations of '*Lev*' but also emit traces of *Man and Gal* (Kourtchev et al., 2011; Fabbri et

605 al., 2008). Recently, Yan et al. (2018) found a significant linear relationship between ^{14}C-

606 based fossil fraction of WSOC and *Lev-C* in the aerosols generated from coal combustion and

607 the ambient aerosol samples. Therefore, the prevailing linear relationship between OC_{fossil}

608 and *Lev*-C in Gosan samples (Figure 10a) is likely due to a common source contribution from

609 coal combustion in East Asia.

Atmospheric
Chemistry
and Physics
Discussions
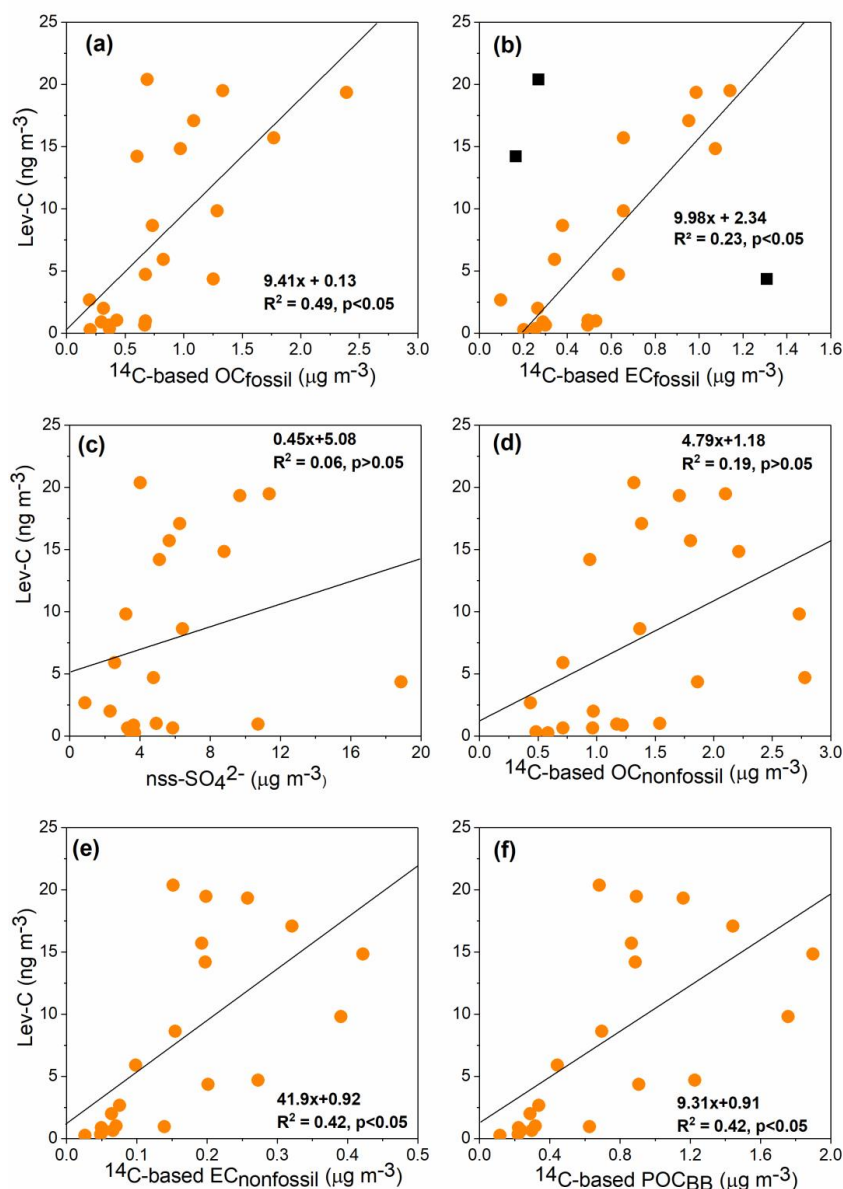
Figure 10. Linear regression analysis between levoglucosan in terms of their carbon content (*Lev*-C) and ^{14}C-based mass concentrations of (a) organic carbon and (b) elemental carbon from fossil origin (OC_{fossil} and EC_{fossil}, respectively), (c) nss-SO_4^{2-}, (d) nonfossil derived organic carbon ($OC_{nonfossil}$), (e) nonfossil derived elemental carbon ($EC_{nonfossil}$), and (f) biomass burning derived primary OC (POC_{BB}) in TSP collected over Gosan during April 2013-April 2014. In panel (b), the squares represent three outliers (i.e., samples with rather high and low *Lev*/EC ratios; please see text for more discussion).

Atmospheric
Chemistry
and Physics
Discussions

618   The slope of the linear regression between *Lev-C* and OC_{fossil} (0.0094; Figure 10a) is

619   higher than those documented for the coal combustion source in China (~0.004±0.007) (Yan

620   et al., 2018). Moreover, *Lev-C* moderately correlated with the EC_{fossil} with the regression

621   slope (~0.01) in Gosan samples (Figure 10b), being comparable to that observed for the coal

622   combustion in China (0.044±0.076) (Yan et al., 2018). It should be noted that excluding the

623   three outlier as shown in Figure 10b (black square), *Lev-C* showed stronger correlation with

624   EC_{fossil} ($R^2 = 0.74$, $p < 0.05$). Of these, two outliers in winter (KOS995: 22-29 January 2014;

625   KOS996: 21 February - 3 March 2014) have higher *Lev-C* levels over that of EC_{fossil}, when

626   air mass trajectories showed the impact of BB emissions in the North China Plain. In

627   contrast, the third outlier in summer (KOS979: 1-11 Jun'2013) has a lower *Lev*-C/EC_{fossil},

628   while air parcel transported from nearby cities in China, Korea and Japan, thus, have more

629   contribution from vehicular emissions. Overall, both the regression slopes are, thus, the

630   representative nature of *Lev*-C/OC_{fossil} and *Lev*-C/EC_{fossil} in the East Asian outflow. *Lev*-C and

631   nss-SO_4^{2-} exhibited a poor correlation (Figure 10c) although both were transported from East

632   Asia.

633   *Lev*-C exhibited a rather weak correlation with $OC_{nonfossil}$ ($R^2 = 0.19$) than that with

634    $EC_{nonfossil}$ ($R^2 = 0.42$) over Gosan during the study period (Figure 10d-e). This could be likely

635   because $OC_{nonfossil}$ has contributions from the BB and the secondary formation process or the

636   primary biogenic sources. The contribution of primary OC generated from BB (POC_{BB}) to

637    $OC_{nonfossil}$ was taken from Zhang et al. (2016). In their study, the ^{14}C-based $EC_{nonfossil}$ levels

638   were scaled by a factor to constrain the POC_{BB} (Zhang et al., 2016). Here the conversion

639   factor is '4.5' (range: 3-10), which is a median value representing the primary OC/EC ratio

640   from BB emissions (($POC/EC)_{BB}$).

641    $$POC_{BB} = EC_{nonfossil} \times (POC/EC)_{BB} \qquad (7)$$

642   *Lev*-C showed a somewhat improved linear correlation with POC_{BB} than with the $OC_{nonfossil}$

643   (Figure 10f). It is apparent from Figure 10 that the regression slopes are somewhat

644   comparable, indicating their contribution to *Lev* from both coal combustion and BB

645   emissions over Gosan.

646   **4. Conclusions**

647   We investigated seasonal variations of primary organic components such as anhydrosugars,

648   primary sugars, and sugar alcohols and biogenic secondary organic aerosol (BSOA) tracers

649   (isoprene- and monoterpene-derived SOA products) in ambient aerosols from Gosan, Jeju

650   Island. Among the detected sugar compounds, levoglucosan was dominant in winter/fall,

651   whereas glucose and sucrose were more abundant in spring/summer. The seasonal trends

652   documented that BB impact is more significant in winter/fall and the primary bioaerosol
653   particles are important in spring/summer. Strong linear relationships of levoglucosan (*Lev*)
654   with galactosan (*Gal*) and mannosan (*Man*) together with their mass ratios of *Lev*/*Gal*
655   (6.7±2.2) and *Lev*/*Man* (15.0±6.7), reflect their contribution from hardwood burning
656   emissions. On a similar note, sucrose showed significant correlations with glucose and
657   fructose, suggesting their origin from airborne pollen. The significant positive linear
658   relationship was found between the fungal spore tracer compounds (i.e., arabitol, mannitol
659   and erythritol) and trehalose (e.g., a proxy for soil organic carbon), implying their
660   contribution from airborne fungal spores and soil microbes in the East Asian outflow. These
661   sugar alcohol tracers are abundantly emitted in summer, followed by fall, spring, and winter.

662   Distributions of biogenic SOA tracers were characterized by a predominance of
663   monoterpene- than isoprene-derived oxidation products in Gosan aerosols. All the BSOA
664   tracers were dominant in summer, followed by fall/spring, and then winter. The low ratio of
665   cis-pinonic acid + pinic acid to MBTCA (P/M) demonstrated that monoterpene SOA was
666   relatively aged over Gosan aerosols. The estimated secondary organic carbon (SOC) with the
667   predominance in summer indicates that substantial SOA formation occurred in summer due
668   to the favorable meteorological conditions. The backward air mass trajectories and source
669   apportionment studies (i.e., linear regressions, diagnostic mass ratios, and positive matrix
670   factorization analysis) entirely demonstrated that BB and biogenic SOA contribution mostly
671   dominate the ambient OA loadings in the East Asian outflow. Interestingly, *Lev-C* exhibited
672   significant positive linear relationships with ^{14}C-based nonfossil and fossil organic carbon
673   fractions along with the comparable regression slopes. This result reveals that BB and coal
674   (lignite) combustion both are important source for levoglucosan in the East Asian outflow.

675   Although there is some evidence that *Lev* could originate from the combustion of
676   brown coals (*e.g.,* lignite) in China; however, our observations are from the KCOG (receptor
677   site) also hinted for the fossil source contribution of this molecular marker in the regional
678   influx of the East Asian outflow. Therefore, attribution of ambient *Lev* levels over the WNP
679   to the impact of BB emission may cause large uncertainty.

680   **Data availability**
681   The data used in this paper are available upon the request from the corresponding author.

682   **Author contributions**
683   YLZ and KK designed the research. ML collected the aerosol samples. MMH and SB
684   performed the analysis of aerosol samples. MMH wrote the paper under the guidance of YLZ
685   and KK. All authors were actively involved in the discussion of the paper.

Atmospheric
Chemistry
and Physics
Discussions

693 **References**

694 Arimoto, R., Duce, R. A., Savoie, D. L., Prospero, J. M., Talbot, R., Cullen, J. D., Tomza, U.,
695   Lewis, N. F., and Ray, B. J.: Relationships among aerosol constituents from Asia and the
696   North Pacific during PEM-West A, J. Geophys. Res. Atmos., 101, 2011-2023,
697   https://doi.org/10.1029/95JD01071, 1996.

698 Athanasopoulou, E., Tombrou, M., Russell, A. G., Karanasiou, A., Eleftheriadis, K., and
699   Dandou, A.: Implementation of road and soil dust emission parameterizations in the
700   aerosol model CAMx: Applications over the greater Athens urban area affected by natural
701   sources, J. Geophys. Res., 115, D17301, https://doi.org/10.1029/2009JD013207, 2010.

702 Bauer, H., Claeys, M., Vermeylen, R., Schueller, E., Weinke, G., Berger, A., and Puxbaum,
703   H.: Arabitol and mannitol as tracers for the quantification of airborne fungal spores,
704   Atmos. Environ., 42, 588–593, 2008.

705 Bikkina, S., Haque, M. M., Sarin, M., and Kawamura, K.: Tracing the relative significance of
706   primary versus secondary organic aerosols from biomass burning plumes over coastal
707   ocean using sugar compounds and stable carbon isotopes, ACS Earth Space Chem., 3,
708   1471-1484, https://doi.org/10.1021/acsearthspacechem.9b00140, 2019.

709 Bikkina, S., Kawamura, K., Sakamoto, Y., and Hirokawa, J: Low molecular weight
710   dicarboxylic acids, oxocarboxylic acids and α-dicarbonyls as ozonolysis products of
711   isoprene: Implication for the gaseous-phase formation of secondary organic aerosols, Sci.
712   Total Environ., 769, 144472, https://doi.org/10.1016/j.scitotenv.2020.144472, 2021.

713 Brahney, J., Ballantyne, A. P., Sievers, C., and Neff, J. C.: Increasing Ca^{2+} deposition in the
714   western US: The role of mineral aerosols, Aeolian Res., 10, 77–87, 2013.

715 Broadgate, W. J., Liss, P. S., and Penkett, S. A.: Seasonal emissions of isoprene and other
716   reactive hydrocarbon gases from the ocean, Geophys. Res. Lett., 24, 2675-2678,
717   https://doi.org/10.1029/97GL02736, 1997.

718 Cheng, Y., Engling, G., He, K.-B., Duan, F.-K., Ma, Y.-L., Du, Z.-Y., Liu, J.-M., Zheng, M.,
719   and Weber, R. J.: Biomass burning contribution to Beijing aerosol, Atmos. Chem. Phys.,
720   13, 7765–7781, 2013.

721 Claeys, M., Graham, B., Vas, G., Wang, W., Vermeylen, R., Pashynska, V., Cafmeyer, J.,
722   Guyon, P., Andreae, M. O., Artaxo, P., and Maenhaut, W.: Formation of secondary
723   organic aerosols through photooxidation of isoprene, Science, 303(5661), 1173–1176,
724   2004.

725 Claeys, M., Szmigielski, R., Kourtchev, I., van der Veken, P., Vermeylen, R., Maenhaut, W.,
726   Jaoui, M., Kleindienst, T. E., Lewandowski, M., Offenberg, J., and Edney, E. O.:

727   Hydroxydicarboxylic acids: Markers for secondary organic aerosol from the
728   photooxidation of α-pinene, Environ. Sci. Technol., 41(5), 1628–1634, 2007.
729 Conte, L., Szopa, S., Aumont, O., Gros, V., and Bopp, L.: Sources and sinks of isoprene in
730   the global open ocean: Simulated patterns and emissions to the atmosphere, J. Geophys.
731   Res. Ocean., 9, e2019JC015946, https://doi.org/10.1029/2019JC015946, 2020.
732 Deguillaume, L., Leriche, M., Amato, P., Ariya, P. A., Delort, A.-M., Pöschl, U.,
733   Chaumerliac, N., Bauer, H., Flossmann, A. I., and Morris, C. E.: Microbiology and
734   atmospheric processes: chemical interactions of primary biological aerosols,
735   Biogeosciences, 5, 1073–1084, 2008.
736 Ding, X., Wang, X. M., Gao, B., Fu, X. X., He, Q. F., Zhao, X. Y., Yu, J. Z., and Zheng, M.:
737   Tracer-based estimation of secondary organic carbon in the Pearl River Delta, south
738   China, J. Geophys. Res. Atmos., 117, D05313, https://doi.org/10.1029/2011JD016596,
739   2012.
740 Ding, X., He, Q. F., Shen, R. Q., Yu, Q. Q., and Wang, X. M.: Spatial distributions of
741   secondary organic aerosols from isoprene, monoterpenes, β-caryophyllene, and aromatics
742   over China during summer, J. Geophys. Res., 119, 11877-11891,
743   https://doi.org/10.1002/2014JD021748, 2014.
744 Engling, G., Carrico, C. M., Kreldenweis, S. M., Collett, J. L., Day, D. E., Malm, W. C.,
745   Lincoln, E., Hao, W. M., Iinuma, Y., and Herrmann, H.: Determination of levoglucosan
746   in biomass combustion aerosol by high-performance anion-exchange chromatography
747   with pulsed amperometric detection, Atmos. Environ., 40, S299–S311, 2006.
748 Engling, G., Lee, J. J., Tsai, Y. W., Lung, S. C. C., Chou, C. C. K., and Chan, C. Y.: Size-
749   resolved anhydrosugar composition in smoke aerosol from controlled field burning of rice
750   straw, Aerosol Sci. Technol., 43(7), 662–672,
751   https://doi.org/10.1080/02786820902825113, 2009.
752 Fabbri, D., Marynowski, L., Fabianska, M. J., Zaton, M., and Simoneit, B. R. T.:
753   Levoglucosan and other cellulose markers in pyrolysates of miocene lignites:
754   Geochemical and environmental implications, Environ. Sci. Technol., 42(8), 2957–2963,
755   https://doi.org/10.1021/Es7021472, 2008.
756 Fine, P. M., Cass, G. R., and Simoneit, B. R. T.: Chemical characterization of fine particle
757   emissions from fireplace combustion of woods grown in the northeastern United States,
758   Environ. Sci. Technol., 35(13), 2665–2675, 2001.
759 Fine, P. M., Cass, G. R., and Simoneit, B. R. T.: Chemical characterization of fine particle
760   emissions from the fireplace combustion of wood types grown in the Midwestern and
761   Western United States, Environ. Eng. Sci., 21(3), 387–409, 2004.
762 Fraser, M. P. and Lakshmanan, K.: Using levoglucosan as a molecular marker for the long-
763   range transport of biomass combustion aerosols, Environ. Sci. Technol., 34(21), 4560–
764   4564, https://doi.org/10.1021/es991229l, 2000.
765 Fu, P., Kawamura, K., Kanaya, Y., and Wang, Z.: Contributions of biogenic volatile organic
766   compounds to the formation of secondary organic aerosols over Mt. Tai, Central East
767   China, Atmos. Environ., 44, 4817-4826, https://doi.org/10.1016/j.atmosenv.2010.08.040,
768   2010a.
769 Fu, P., Kawamura, K., Kobayashi, M., and Simoneit, B. R. T.: Seasonal variations of sugars
770   in atmospheric particulate matter from Gosan, Jeju Island: Significant contributions of

771   airborne pollen and Asian dust in spring, Atmos. Environ., 55, 234–239,
772   https://doi.org/10.1016/j.atmosenv.2012.02.061, 2012a.
773   Fu, P. Q., Kawamura, K., Okuzawa, K., Aggarwal, S. G., Wang, G., Kanaya, Y., and Wang,
774   Z.: Organic molecular compositions and temporal variations of summertime mountain
775   aerosols over Mt. Tai, North China Plain, J. Geophys. Res. Atmos., 113, D1910,
776   https://doi.org/10.1029/2008JD009900, 2008.
777   Fu, P. Q., Kawamura, K., and Barrie, L. A.: Photochemical and other sources of organic
778   compounds in the Canadian high Arctic aerosol pollution during winter-spring, Environ.
779   Sci. Technol., 43(2), 286–292, 2009a.
780   Fu, P. Q., Kawamura, K., Chen, J., and Barrie, L. A.: Isoprene, monoterpene, and
781   sesquiterpene oxidation products in the high Arctic aerosols during late winter to early
782   summer, Environ. Sci. Technol., 43(11), 4022–4028, 2009b.
783   Fu, P. Q., Kawamura, K., Pavuluri, C. M., Swaminathan, T., and Chen, J.: Molecular
784   characterization of urban organic aerosol in tropical India: contributions of primary
785   emissions and secondary photooxidation, Atmos. Chem. Phys., 10(6), 2663–2689, 2010b.
786   Fu, P. Q., Kawamura, K., and Miura, K.: Molecular characterization of marine organic
787   aerosols collected during a round-the-world cruise, J. Geophys. Res., 116, D13302,
788   https://doi.org/10.1029/2011jd015604, 2011.
789   Fu, P. Q., Kawamura, K., Chen, J., Li, J., Sun, Y. L., Liu, Y., Tachibana, E., Aggarwal, S. G.,
790   Okuzawa, K., Tanimoto, H., Kanaya, Y., and Wang, Z. F.: Diurnal variations of organic
791   molecular tracers and stable carbon isotopic composition in atmospheric aerosols over
792   Mt. Tai in the North China Plain: an influence of biomass burning, Atmos. Chem. Phys.,
793   12(18), 8359–8375, https://doi.org/10.5194/Acp-12-8359-2012, 2012b.
794   Gómez-González, Y., Wang, W., Vermeylen, R., Chi, X., Neirynck, J., Janssens, I. A.,
795   Maenhaut, W., and Claeys, M.: Chemical characterisation of atmospheric aerosols during
796   a 2007 summer field campaign at Brasschaat, Belgium: Sources and source processes of
797   biogenic secondary organic aerosol, Atmos. Chem. Phys., 12, 125-138,
798   https://doi.org/10.5194/acp-12-125-2012, 2012.
799   Graham, B., Guyon, P., Taylor, P. E., Artaxo, P., Maenhaut, W., Glovsky, M. M., Flagan, R.
800   C., and Andreae, M. O.: Organic compounds present in the natural Amazonian aerosol:
801   Characterization by gas chromatography-mass spectrometry, J. Geophys. Res. Atmos.,
802   108, D24, 4766, https://doi.org/10.1029/2003JD003990, 2003.
803   Griffin, R. J., Cocker, D. R., Seinfeld, J. H., and Dabdub, D.: Estimate of global atmospheric
804   organic aerosol from oxidation of biogenic hydrocarbons, Geophys. Res. Lett., 26, 2721–
805   2724, 1999.
806   Guenther, A., Hewitt, C. N., Erickson, D., Fall, R., Geron, C., Graedel, T., Harley, P.,
807   Klinger, L., Lerdau, M., McKay, W. A., Pierce, T., Scholes, B. R. S., Tallamraju, R.,
808   Taylor, J., and Zimmerman, P.: A global model of natural volatile organic compound
809   emissions, J. Geophys. Res., 100(D5), 8873–8892, 1995.
810   Guenther, A., Karl, T., Harley, P., Wiedinmyer, C., Palmer, P. I., and Geron, C.: Estimates of
811   global terrestrial isoprene emissions using MEGAN (Model of Emissions of Gases and
812   Aerosols from Nature), Atmos. Chem. Phys., 6, 3181–3210, 2006.
813   Haque, M. M., Kawamura, K., Deshmukh, D. K., Fang, C., Song, W., Mengying, B., and
814   Zhang, Y. L.: Characterization of organic aerosols from a Chinese megacity during

815   winter: Predominance of fossil fuel combustion, Atmos. Chem. Phys., 19, 5147-5164,
816   https://doi.org/10.5194/acp-19-5147-2019, 2019.
817   Heald, C. L., Henze, D. K., Horowitz, L. W., Feddema, J., Lamarque, J. F., Guenther, A.,
818   Hess, P. G., Vitt, F., Seinfeld, J. H., Goldstein, A. H., and Fung, I.: Predicted change in
819   global secondary organic aerosol concentrations in response to future climate, emissions,
820   and land use change, J. Geophys. Res., 113(D5), https://doi.org/10.1029/2007jd009092,
821   2008.
822   Hu, Q. H., Xie, Z. Q., Wang, X. M., Kang, H., He, Q. F., and Zhang, P.: Secondary organic
823   aerosols over oceans via oxidation of isoprene and monoterpenes from Arctic to
824   Antarctic, Sci. Rep., 3, 3119, https://doi.org/10.1038/srep02280, 2013.
825   Huebert, B. J., Bates, T., Russell, P. B., Shi, G. Y., Kim, Y. J., Kawamura, K., Carmichael,
826   G., and Nakajima, T.: An overview of ACE-Asia: Strategies for quantifying the
827   relationships between Asian aerosols and their climatic impacts, J. Geophys. Res. Atmos.,
828   108(D23), 8633, https://doi.org/10.1029/2003JD003550, 2003.
829   Jia, Y. L. and Fraser, M.: Characterization of saccharides in size-fractioned ambient
830   particulate matter and aerosol sources: The contribution of primary biological aerosol
831   particles (PBAPs) and soil to ambient particulate matter, Environ. Sci. Technol., 45(3),
832   930–936, https://doi.org/10.1021/es103104e, 2011.
833   Kanakidou, M., Seinfeld, J. H., Pandis, S. N., Barnes, I., Dentener, F. J., Facchini, M. C., Van
834   Dingenen, R., Ervens, B., Nenes, A., Nielsen, C. J., Swietlicki, E., Putaud, J. P.,
835   Balkanski, Y., Fuzzi, S., Horth, J., Moortgat, G. K., Winterhalter, R., Myhre, C. E. L.,
836   Tsigaridis, K., Vignati, E., Stephanou, E. G., and Wilson, J.: Organic aerosol and global
837   climate modelling: a review, Atmos. Chem. Phys., 5, 1053–1123, 2005.
838   Kang, M., Ren, L., Ren, H., Zhao, Y., Kawamura, K., Zhang, H., Wei, L., Sun, Y., Wang, Z.,
839   and Fu, P.: Primary biogenic and anthropogenic sources of organic aerosols in Beijing,
840   China: Insights from saccharides and n-alkanes, Environ. Pollut., 243, 1579-1587,
841   https://doi.org/10.1016/j.envpol.2018.09.118, 2018a.
842   Kang, M., Fu, P., Kawamura, K., Yang, F., Zhang, H., Zang, Z., Ren, H., Ren, L., Zhao, Y.,
843   Sun, Y., and Wang, Z.: Characterization of biogenic primary and secondary organic
844   aerosols in the marine atmosphere over the East China Sea, Atmos. Chem. Phys., 19,
845   13947-13967, https://doi.org/10.5194/acp-18-13947-2018, 2018b.
846   Kawamura, K., Kobayashi, M., Tsubonuma, N., Mochida, M., Watanabe, T., and Lee, M.:
847   Organic and inorganic compositions of marine aerosols from East Asia: Seasonal
848   variations of water-soluble dicarboxylic acids, major ions, total carbon and nitrogen, and
849   stable C and N isotopic composition, in geochemical investigations in earth and space
850   science: A Tribute to Isaac R. Kaplan, edited by R. J. Hill, J. Leventhal, Z. Aizenshtat, M.
851   J. Baedecker, G. Claypool, R. Eganhouse, M. Goldhaber, and K. Peters, pp. 243–265, The
852   Geochemical Society, 2004.
853   Kessler, S. H., Smith, J. D., Che, D. L., Worsnop, D. R., Wilson, K. R., and Kroll, J. H.:
854   Chemical sinks of organic aerosol: Kinetics and products of the heterogeneous oxidation
855   of erythritol and levoglucosan, Environ. Sci. Technol., 44(18), 7005–7010,
856   https://doi.org/10.1021/Es101465m, 2010.
857   Kourtchev, I., Hellebust, S., Bell, J. M., O'Connor, I. P., Healy, R. M., Allanic, A., Healy, D.,
858   Wenger, J. C., and Sodeau, J. R.: The use of polar organic compounds to estimate the

Atmospheric
Chemistry
and Physics
Discussions

30

859   contribution of domestic solid fuel combustion and biogenic sources to ambient levels of
860   organic carbon and $PM_{2.5}$ in Cork Harbour, Ireland, Sci. Total Environ., 11, 2143-2155,
861   https://doi.org/10.1016/j.scitotenv.2011.02.027, 2011.
862 Kroll, J. H., Ng, N. L., Murphy, S. M., Flagan, R. C., and Seinfeld, J. H.: Secondary organic
863   aerosol formation from isoprene photooxidation under high-NOx conditions, Geophys.
864   Res. Lett., 32(18), L18808, https://doi.org/10.1029/2005gl023637, 2005.
865 Kroll, J. H., Ng, N. L., Murphy, S. M., Flagan, R. C., and Seinfeld, J. H.: Secondary organic
866   aerosol formation from isoprene photooxidation, Environ. Sci. Technol., 40, 1869–1877,
867   2006.
868 Kundu, S., Kawamura, K., and Lee, M.: Seasonal variations of diacids, ketoacids, and α-
869   dicarbonyls in aerosols at Gosan, Jeju Island, South Korea: Implications for sources,
870   formation, and degradation during long-range transport, J. Geophys. Res., 115, D19307,
871   https://doi.org/10.1029/2010jd013973, 2010.
872 Lewis, D. H. and Smith, D. C.: Sugar alcohols (polyols) in fungi and green plants: 1.
873   Distributions, physiology and metabolism, New Phytol., 66, 143–184, 1967.
874 Liu, J., Chu, B., Chen, T., Liu, C., Wang, L., Bao, X., and He, H.: Secondary organic aerosol
875   formation from ambient air at an urban site in Beijing: Effects of OH exposure and
876   precursor concentrations, Environ. Sci. Technol., 52, 6834-6841,
877   https://doi.org/10.1021/acs.est.7b05701, 2018.
878 Medeiros, P. M. and Simoneit, B. R. T.: Analysis of sugars in environmental samples by gas
879   chromatography-mass spectrometry, J. Chromatogr. A, 1141(2), 271–278,
880   https://doi.org/10.1016/j.chroma.2006.12.017, 2007.
881 Medeiros, P. M., Conte, M. H., Weber, J. C., and Simoneit, B. R. T.: Sugars as source
882   indicators of biogenic organic carbon in aerosols collected above the Howland
883   Experimental Forest, Maine, Atmos. Environ., 40(9), 1694–1705, 2006.
884 Mohn, J., Szidat, S., Fellner, J., Rechberger, H., Quartier, R., Buchmann, B., and
885   Emmenegger, L.: Determination of biogenic and fossil CO_2 emitted by waste incineration
886   based on $^{14}CO_2$ and mass balances, Bioresour. Technol., 99, 6471-6479,
887   https://doi.org/10.1016/j.biortech.2007.11.042, 2008.
888 Müller, L., Reinnig, M. C., Naumann, K. H., Saathoff, H., Mentel, T. F., Donahue, N. M.,
889   and Hoffmann, T.: Formation of 3-methyl-1,2,3-butanetricarboxylic acid via gas phase
890   oxidation of pinonic acid - A mass spectrometric study of SOA aging, Atmos. Chem.
891   Phys., 12, 1483-1496, https://doi.org/10.5194/acp-12-1483-2012, 2012.
892 Nakajima, T., Yoon, S. C., Ramanathan, V., Shi, G. Y., Takemura, T., Higurashi, A.,
893   Takamura, T., Aoki, K., Sohn, B. J., Kim, S. W., Tsuruta, H., Sugimoto, N., Shimizu, A.,
894   Tanimoto, H., Sawa, Y., Lin, N. H., Lee, C. T., Goto, D., and Schutgens, N.: Overview of
895   the atmospheric brown cloud east Asian regional experiment 2005 and a study of the
896   aerosol direct radiative forcing in east Asia, J. Geophys. Res. Atmos., 112, D24S91,
897   https://doi.org/10.1029/2007JD009009, 2007.
898 Ng, N. L., Kwan, A. J., Surratt, J. D., Chan, A. W. H., Chhabra, P. S., Sorooshian, A., Pye, H.
899   O. T., Crounse, J. D., Wennberg, P. O., Flagan, R. C., and Seinfeld, J. H.: Secondary
900   organic aerosol (SOA) formation from reaction of isoprene with nitrate radicals (NO_3),
901   Atmos. Chem. Phys., 8(14), 4117–4140, 2008.

902 Offenberg, J., Lewis, C., Lewandowski, M., Jaoui, M., Kleindienst, T. E., and Edney, E. O.:
903   Contributions of toluene and α-pinene to SOA formed in an irradiated toluene/r-
904   pinene/NOx/air mixture: Comparison of results using ^{14}C content and SOA organic tracer
905   methods, Environ. Sci. Tec., 41, 3972–3976, 2007.
906 Pio, C., Legrand, M., Alves, C. A., Oliveira, T., Afonso, J., Caseiro, A., Puxbaum, H.,
907   Sánchez-Ochoa, A., and Gelencsér, A.: Chemical composition of atmospheric aerosols
908   during the 2003 summer intense forest fire period, Atmos. Environ., 42, 7530–7543,
909   2008.
910 Ramanathan, V., Li, F., Ramana, M. V., Praveen, P. S., Kim, D., Corrigan, C. E., Nguyen, H.,
911   Stone, E. A., Schauer, J. J., Carmichael, G. R., Adhikary, B., and Yoon, S. C.:
912   Atmospheric brown clouds: Hemispherical and regional variations in long-range
913   transport, absorption, and radiative forcing, J. Geophys. Res. Atmos., 112, D22S21,
914   https://doi.org/10.1029/2006JD008124, 2007.
915 Robinson, A. L., Donahue, N. M., Shrivastava, M. K., Weitkamp, E. A., Sage, A. M.,
916   Grieshop, A. P., Lane, T. E., Pierce, J. R., and Pandis, S. N.: Rethinking organic aerosols:
917   Semivolatile emissions and photochemical aging, Science, 315, 1259–1262, 2007.
918 Salazar, G., Zhang, Y. L., Agrios, K., and Szidat, S.: Development of a method for fast and
919   automatic radiocarbon measurement of aerosol samples by online coupling of an
920   elemental analyzer with a MICADAS AMS, Nucl. Instruments Methods Phys. Res. Sect.
921   B Beam Interact. with Mater. Atoms, 361, 163-167,
922   https://doi.org/10.1016/j.nimb.2015.03.051, 2015.
923 Schmidl, C., Marr, I. L., Caseiro, A., Kotianova, P., Berner, A., Bauer, H., Kasper-Giebl, A.,
924   and Puxbaum, H.: Chemical characterisation of fine particle emissions from wood stove
925   combustion of common woods growing in mid-European Alpine regions, Atmos.
926   Environ., 42, 126–141, 2008a.
927 Schmidl, C., Bauer, H., Dattler, A., Hitzenberger, R., Weissenboeck, G., Marr, I. L., and
928   Puxbaum, H.: Chemical characterisation of particle emissions from burning leaves,
929   Atmos. Environ., 42(40), 9070–9079, https://doi.org/10.1016/J.Atmosenv.2008.09.010,
930   2008b.
931 Shaw, S. L., Gantt, B., and Meskhidze, N.: Production and emissions of marine isoprene and
932   monoterpenes: A Review, Adv. Meteorol., 2010, 408696,
933   https://doi.org/10.1155/2010/408696, 2010.
934 Simoneit, B. R. T.: Biomass burning-a review of organic tracers for smoke from incomplete
935   combustion, Appl. Geochem., 17, 129–162, 2002.
936 Simoneit, B. R. T., Elias, V. O., Kobayashi, M., Kawamura, K., Rushdi, A. I., Medeiros, P.
937   M., Rogge, W. F., and Didyk, B. M.: Sugars-dominant water-soluble organic compounds
938   in soils and characterization as tracers in atmospheric particulate matter, Environ. Sci.
939   Technol., 38(22), 5939–5949, 2004a.
940 Simoneit, B. R. T., Kobayashi, M., Mochida, M., Kawamura, K., Lee, M., Lim, H-J., Turpin,
941   B. J., and Komazaki, Y.: Composition and major sources of organic compounds of
942   aerosol particulate matter sampled during the ACE-Asia campaign, J. Geophys. Res.,
943   109(D19), D19S10, https://doi.org/10.1029/2004jd004598, 2004b.
944 Simoneit, B. R. T., Schauer, J. J., Nolte, C. G., Oros, D. R., Elias, V. O., Fraser, M. P.,
945   Rogge, W. F., and Cass, G. R.: Levoglucosan, a tracer for cellulose in biomass burning

Atmospheric
Chemistry
and Physics
Discussions

946 and atmospheric particles, Atmos. Environ., 33(2), 173–182,
947 https://doi.org/10.1016/S1352-2310(98)00145-9, 1999.

948 Singh, N., Mhawish, A., Deboudt, K., Singh, R. S., and Banerjee, T.: Organic aerosols over
949 Indo-Gangetic Plain: Sources, distributions and climatic implications, Atmos. Environ.,
950 157, 59-74, https://doi.org/10.1016/j.atmosenv.2017.03.008, 2017.

951 Stein, A. F., Draxler, R. R., Rolph, G. D., Stunder, B. J. B., Cohen, M. D., and Ngan, F.:
952 Noaa's hysplit atmospheric transport and dispersion modeling system, Bull. Am.
953 Meteorol. Soc., 96, 2059-2077, https://doi.org/10.1175/BAMS-D-14-00110.1, 2015.

954 Stuiver, M. and Polach, H. A.: Discussion: Reporting of ^{14}C data, Radiocarbon, 19(3),
955 355−363, 1997.

956 Sullivan, A. P., Holden, A. S., Patterson, L. A., McMeeking, G. R., Kreidenweis, S. M.,
957 Malm, W. C., Hao, W. M., Wold, C. E., and Collett, Jr., J. L.: A method for smoke
958 marker measurements and its potential application for determining the contribution of
959 biomass burning from wildfires and prescribed fires to ambient $PM_{2.5}$ organic carbon, J.
960 Geophys. Res., 113, D22302, https://doi.org/10.1029/2008JD010216, 2008.

961 Surratt, J. D., Murphy, S. M., Kroll, J. H., Ng, N. L., Hildebrandt, L., Sorooshian, A.,
962 Szmigielski, R., Vermeylen, R., Maenhaut, W., Claeys, M., Flagan, R. C., and Seinfeld, J.
963 H.: Chemical composition of secondary organic aerosol formed from the photooxidation
964 of isoprene, J. Phys. Chem. A, 110(31), 9665–9690, 2006.

965 Surratt, J. D., Chan, A. W. H., Eddingsaas, N. C., Chan, M. N., Loza, C. L., Kwan, A. J.,
966 Hersey, S. P., Flagan, R. C., Wennberg, P. O., and Seinfeld, J. H.: Reactive intermediates
967 revealed in secondary organic aerosol formation from isoprene, Proc. Natl. Acad. Sci.
968 USA, 107(15), 6640–6645, 2010.

969 Szidat, S., Jenk, T. M., Synal, H. A., Kalberer, M., Wacker, L., Hajdas, I., Kasper-Giebl, A.,
970 and Baltensperger, U.: Contributions of fossil fuel, biomass-burning, and biogenic
971 emissions to carbonaceous aerosols in Zurich as traced by ^{14}C, J. Geophys. Res. Atmos.,
972 111, D07206, https://doi.org/10.1029/2005JD006590, 2006.

973 Szmigielski, R., Surratt, J. D., Gómez-González, G., Van der Veken, P., Kourtchev, I.,
974 Vermeylen, R., Blockhuys, F., Jaoui, M., Kleindienst, T. E., Lewandowski, M.,
975 Offenberg, J. H., Edney, E. O., Seinfeld, J. H., Maenhaut, W., and Claeys, M.: 3-Methyl-
976 1,2,3-butanetricarboxylic acid: An atmospheric tracer for terpene secondary organic
977 aerosol, Geophys. Res. Lett., 34, L24811, https://doi.org/10.1029/2007GL031338, 2007.

978 Theodosi, C., Panagiotopoulos, C., Nouara, A., Zarmpas, P., Nicolaou, P., Violaki, K.,
979 Kanakidou, M., Sempéré, R., and Mihalopoulos, N.: Sugars in atmospheric aerosols over
980 the Eastern Mediterranean, Prog. Oceanogr., 163, Special Issue: SI, 70-81,
981 https://doi.org/10.1016/j.pocean.2017.09.001, 2018.

982 Tyagi, P., Kawamura, K., Kariya, T., Bikkina, S., Fu, P., and Lee, M.: Tracing atmospheric
983 transport of soil microorganisms and higher plant waxes in the East Asian outflow to the
984 North Pacific Rim by using hydroxy fatty acids: Year-round observations at Gosan, Jeju
985 Island, J. Geophys. Res., 122, 4112-4131, https://doi.org/10.1002/2016JD025496, 2017.

986 Verma, S. K., Kawamura, K., Chen, J., Fu, P., and Zhu, C.: Thirteen years of observations on
987 biomass burning organic tracers over Chichijima Island in the western North Pacific: An
988 outflow region of Asian aerosols, J. Geophys. Res., 120, 4155-4168,
989 https://doi.org/10.1002/2014JD022224, 2015.

Atmospheric
Chemistry
and Physics
Discussions

990　Verma, S. K., Kawamura, K., Chen, J., and Fu, P.: Thirteen years of observations on primary
991　　sugars and sugar alcohols over remote Chichijima Island in the western North Pacific,
992　　Atmos. Chem. Phys., 18, 81-101, https://doi.org/10.5194/acp-18-81-2018, 2018.
993　Wang, G. and Kawamura, K.: Molecular characteristics of urban organic aerosols from
994　　Nanjing: A case study of a mega-city in China, Environ. Sci. Technol., 39(19), 7430–
995　　7438, 2005.
996　Wang, G. H., Kawamura, K., and Lee, M.: Comparison of organic compositions in dust storm
997　　and normal aerosol samples collected at Gosan, Jeju Island, during spring 2005, Atmos.
998　　Environ., 43(2), 219–227, https://doi.org/10.1016/J.Atmosenv.2008.09.046, 2009a.
999　Wang, G. H., Li, J. J., Cheng, C. L., Zhou, B. H., Xie, M. J., Hu, S. Y., Meng, J. J., Sun, T.,
1000　　Ren, Y. Q., Cao, J. J., Liu, S. X., Zhang, T., and Zhao, Z. Z.: Observation of atmospheric
1001　　aerosols at Mt. Hua and Mt. Tai in central and east China during spring 2009-Part 2:
1002　　Impact of dust storm on organic aerosol composition and size distribution, Atmos. Chem.
1003　　Phys., 12(9), 4065–4080, 2012.
1004　Wang, W., Kourtchev, I., Graham, B., Cafmeyer, J., Maenhaut, W., and Claeys, M.:
1005　　Characterization of oxygenated derivatives of isoprene related to 2-methyltetrols in
1006　　Amazonian aerosols using trimethylsilylation and gas chromatography/ion trap mass
1007　　spectrometry, Rapid Commun. Mass Spectrom., 19, 1343–1351, 2005.
1008　Wang, Y. Q., Zhang, X. Y., and Draxler, R. R.: TrajStat: GIS-based software that uses
1009　　various trajectory statistical analysis methods to identify potential sources from long-term
1010　　air pollution measurement data, Environ. Model. Softw., 24, 938-939,
1011　　https://doi.org/10.1016/j.envsoft.2009.01.004, 2009b.
1012　Yan, C., Zheng, M., Sullivan, A. P., Shen, G., Chen, Y., Wang, S., Zhao, B., Cai, S.,
1013　　Desyaterik, Y., Li, X., Zhou, T., Gustafsson, Ö., and Collett, J. L.: Residential coal
1014　　combustion as a source of levoglucosan in China, Environ. Sci. Technol., 52, 3, 1665–
1015　　1674, https://doi.org/10.1021/acs.est.7b05858, 2018.
1016　Yttri, K. E., Dye, C., and Kiss, G.: Ambient aerosol concentrations of sugars and sugar-
1017　　alcohols at four different sites in Norway, Atmos. Chem. Phys., 7, 4267–4279, 2007.
1018　Zangrando, R., Barbaro, E., Kirchgeorg, T., Vecchiato, M., Scalabrin, E., Radaelli, M.,
1019　　Đorđević, D., Barbante, C., and Gambaro, A.: Five primary sources of organic aerosols in
1020　　the urban atmosphere of Belgrade (Serbia), Sci. Total Environ., 571, 1441-1453,
1021　　https://doi.org/10.1016/j.scitotenv.2016.06.188, 2016.
1022　Zhang, Y. L., Perron, N., Ciobanu, V. G., Zotter, P., Minguillón, M. C., Wacker, L., Prévôt,
1023　　A. S. H., Baltensperger, U., and Szidat, S.: On the isolation of OC and EC and the optimal
1024　　strategy of radiocarbon-based source apportionment of carbonaceous aerosols, Atmos.
1025　　Chem. Phys., 12, 10841-10856, https://doi.org/10.5194/acp-12-10841-2012, 2012.
1026　Zhang, Y. L., Huang, R. J., El Haddad, I., Ho, K. F., Cao, J. J., Han, Y., Zotter, P., Bozzetti,
1027　　C., Daellenbach, K. R., Canonaco, F., Slowik, J. G., Salazar, G., Schwikowski, M.,
1028　　Schnelle-Kreis, J., Abbaszade, G., Zimmermann, R., Baltensperger, U., Prévôt, A. S. H.,
1029　　and Szidat, S.: Fossil vs. non-fossil sources of fine carbonaceous aerosols in four Chinese
1030　　cities during the extreme winter haze episode of 2013, Atmos. Chem. Phys., 15(3), 1299-
1031　　1312, https://doi.org/10.5194/acp-15-1299-2015, 2015.
1032　Zhang, Y. L., Kawamura, K., Agrios, K., Lee, M., Salazar, G., and Szidat, S.: Fossil and
1033　　nonfossil sources of organic and elemental carbon aerosols in the outflow from Northeast

1034   China, Environ. Sci. Technol., 50, 6284-6292, https://doi.org/10.1021/acs.est.6b00351,
1035   2016.
1036 Zhu, C., Kawamura, K., and Kunwar, B.: Effect of biomass burning over the western North
1037   Pacific Rim: wintertime maxima of anhydrosugars in ambient aerosols from Okinawa.,
1038   Atmos. Chem. Phys., 15, 1959–1973, https://doi.org/10.5194/acp-15-1959-2015, 2015a.
1039 Zhu, C., Kawamura, K., and Kunwar, B.: Organic tracers of primary biological aerosol
1040   particles at subtropical Okinawa island in the western North pacific rim, J. Geophys. Res.,
1041   120, 5504-5523, https://doi.org/10.1002/2015JD023611, 2015b.

1042

1043

1044

1045

1046

1047

1048

1049

1050

1051

1052

1053

1054

1055

1056

1057

1058

1059

1060

1061

Atmospheric
Chemistry
and Physics
Discussions

1062   **Table 1.** Concentrations of identified sugar compounds and BSOA tracers (ng m^{-3}) in the atmospheric
1063   aerosol samples from Gosan.

Species	Annual	Summer	Fall	Winter	Spring
	Avg.[a] ± S.D.[b] Min.[c], Max.[d]	Avg. ± S.D. Min., Max.	Avg. ± S.D. Min., Max.	Avg. ± S.D. Min., Max.	Avg. ± S.D. Min., Max.
Anhydrosugars					
Levoglucosan (Lev)	17.6 ± 16.8 0.60, 45.9	2.92 ± 3.89 0.60, 9.81	21.7 ± 19.0 2.30, 43.9	39.2 ± 6.60 32.0, 45.9	12.7 ± 11.6 1.45, 33.4
Mannosan (Man)	1.57 ± 1.82 0.05, 6.74	0.18 ± 0.24 0.05, 0.61	1.69 ± 1.49 0.13, 3.66	3.63 ± 2.28 1.47, 6.74	1.31 ± 1.57 0.08, 4.08
Galactosan (Gal)	2.28 ± 2.10 0.14, 6.78	0.64 ± 0.68 0.14, 1.82	2.45 ± 2.13 0.35, 4.92	5.21 ± 1.64 3.40, 6.78	1.65 ± 1.26 0.50, 3.88
Primary Sugars					
Glucose	18.8 ± 27.1 2.45, 122	13.4 ± 18.2 2.45, 45.6	16.5 ± 15.7 2.68, 33.6	4.74 ± 3.14 2.88, 9.44	32.4 ± 41.1 4.87, 122
Fructose	10.3 ± 15.9 0.97, 74.0	4.90 ± 5.15 0.97, 13.7	7.48 ± 6.99 1.71, 16.2	3.82 ± 4.45 1.56, 10.5	19.8 ± 25.0 2.69, 74.0
Sucrose	16.1 ± 32.2 0.26, 140	1.46 ± 1.05 0.68, 3.28	9.74 ± 12.1 0.76, 27.2	8.87 ± 16.3 0.42, 33.3	35.1 ± 50.5 0.26, 140
Trehalose	2.42 ± 1.97 0.65, 7.03	2.72 ± 2.53 0.97, 6.98	3.71 ± 2.29 1.18, 7.03	1.21 ± 0.42 0.72, 1.63	1.98 ± 1.55 0.65, 5.33
Xylose	0.81 ± 0.65 0.04, 2.03	0.23 ± 0.23 0.04, 0.63	0.86 ± 0.68 0.14, 1.70	1.59 ± 0.37 1.21, 2.03	0.74 ± 0.55 0.16, 1.68
Sugar alcohols					
Arabitol	3.96 ± 4.24 0.47, 18.7	5.64 ± 7.46 1.20, 18.7	5.27 ± 3.51 2.27, 10.9	1.06 ± 0.60 0.47, 1.91	3.47 ± 2.19 1.18, 6.30
Mannitol	4.61 ± 5.54 0.25, 22.0	7.39 ± 8.65 1.71, 22.0	6.64 ± 6.03 1.69, 16.7	0.99 ± 0.45 0.55, 1.60	3.24 ± 2.67 0.25, 7.03
Erythritol	0.62 ± 0.43 0.12, 1.52	0.92 ± 0.53 0.42, 1.52	0.93 ± 0.33 0.55, 1.27	0.42 ± 0.27 0.16, 0.80	0.30 ± 0.12 0.12, 0.48
Inositol	0.34 ± 0.39 0.04, 1.53	0.29 ± 0.41 0.08, 1.03	0.56 ± 0.60 0.10, 1.53	0.13 ± 0.07 0.08, 0.23	0.35 ± 0.28 0.04, 0.73
Isoprene SOA tracers					
2-MGA	0.99 ± 0.70 0.17, 2.79	1.61 ± 1.17 0.17, 2.79	0.95 ± 0.43 0.51, 1.61	0.67 ± 0.14 0.49, 0.81	0.76 ± 0.35 0.20, 1.32
Σ2-MLTs	1.04 ± 1.40 0.05, 5.81	2.48 ± 1.98 0.51, 5.81	1.34 ± 1.16 0.33, 2.74	0.20 ± 0.05 0.15, 0.26	0.29 ± 0.25 0.05, 0.82
ΣC5-alkene triols	0.20 ± 0.25 0.02, 1.17	0.46 ± 0.44 0.02, 1.17	0.13 ± 0.05 0.05, 0.18	0.09 ± 0.03 0.05, 0.13	0.14 ± 0.11 0.02, 0.30
Monoterpene SOA tracers					
cis-pinonic acid	0.15 ± 0.14 0.02, 0.52	0.12 ± 0.13 0.03, 0.36	0.08 ± 0.06 0.02, 0.16	0.07 ± 0.03 0.02, 0.10	0.26 ± 0.17 0.08, 0.52
pinic acid	1.67 ± 1.01 0.72, 4.81	2.40 ± 1.67 0.99, 4.81	1.53 ± 0.57 0.75, 2.11	1.07 ± 0.25 0.84, 1.42	1.61 ± 0.78 0.72, 2.94
3-HGA	2.30 ± 2.38 0.19, 10.6	3.46 ± 4.39 0.19, 10.6	1.52 ± 0.77 0.76, 2.79	1.40 ± 0.39 0.94, 1.88	2.54 ± 1.83 0.38, 4.57
MBTCA	5.11 ± 4.54 0.29, 19.6	8.44 ± 6.88 3.00, 19.6	6.24 ± 3.64 1.17, 9.49	1.90 ± 0.85 0.97, 2.83	3.77 ± 2.96 0.29, 8.08

[a]Average, [b]Standard deviation, [c]Minimum, [d]Maximum. 2-MGA: 2-methylglyceric acid, 2-MLTs: 2-methyltetrols, 3-HGA: 3-hydroxyglutaric acid, MBTCA: 3-methyl-1,2,3-butanetricarboxylic acid.

1064

Atmospheric
Chemistry
and Physics
Discussions

Open Access

EGU

36

1065 **Table 2.** Statistical summary of diagnostic ratios and carbonaceous components contribution in Gosan
1066 aerosols.
1067

Species	Annual	Summer	Fall	Winter	Spring
	Avg.[a] ± S.D.[b] Min.[c], Max.[d]	Avg. ± S.D. Min., Max.	Avg. ± S.D. Min., Max.	Avg. ± S.D. Min., Max.	Avg. ± S.D. Min., Max.
Diagnostic ratios					
Lev/Man	15.1 ± 6.76 6.81, 31.3	17.1 ± 8.21 8.58, 28.4	13.7 ± 2.51 11.1, 17.3	13.5 ± 6.24 6.81, 21.7	15.4 ± 8.76 6.98, 31.3
Man/Gal	0.55 ± 0.32 0.10, 1.07	0.28 ± 0.13 0.10, 0.42	0.64 ± 0.20 0.37, 0.90	0.66 ± 0.27 0.43, 1.05	0.61 ± 0.43 0.16, 1.07
Lev/K^+ × 10^{-2}	5.73 ± 5.65 0.65, 23.2	1.00 ± 0.52 0.65, 1.91	3.94 ± 2.51 1.26, 6.30	12.3 ± 7.87 6.42, 23.2	6.65 ± 4.48 1.77, 15.3
Lev/OC × 10^{-2}	0.73 ± 0.66 0.08, 2.29	0.14 ± 0.10 0.08, 0.31	0.84 ± 0.61 0.12, 1.56	1.60 ± 0.67 0.99, 2.29	0.56 ± 0.40 0.11, 1.05
Lev/WSOC × 10^{-2}	1.09 ± 0.97 0.10, 3.46	0.20 ± 0.13 0.10, 0.42	1.25 ± 0.94 0.23, 2.21	2.33 ± 0.90 1.48, 3.46	0.92 ± 0.65 0.13, 1.69
MGA/MLTs	2.18 ± 1.59 0.33, 5.40	0.67 ± 0.43 0.33, 1.33	1.04 ± 0.49 0.41, 1.55	3.60 ± 1.43 1.90, 5.40	3.27 ± 1.17 1.60, 4.75
[e]P/MBTCA	0.62 ± 0.61 0.17, 5.90	3.22 ± 0.62 2.47, 3.89	3.62 ± 1.67 1.52, 5.90	1.68 ± 0.64 0.83, 2.38	1.73 ± 1.07 0.34, 3.32
Carbonaceous components					
Isoprene derived SOC (μgC m^{-3})	23.7 ± 23.9 2.26, 97.4	51.0 ± 32.4 8.08, 97.4	25.9 ± 17.9 8.54, 45.7	8.52 ± 1.07 7.46, 9.87	11.3 ± 6.80 2.26, 24.9
Isoprene SOC to OC (%)	1.45 ± 1.74 0.21, 6.40	3.56 ± 2.18 1.03, 6.40	1.46 ± 1.38 0.35, 3.48	0.35 ± 0.17 0.21, 0.57	0.57 ± 0.38 0.24, 1.35
Isoprene SOC to total SOC (%)	35.5 ± 15.5 13.5, 71.1	46.6 ± 20.3 26.0, 71.1	38.1 ± 10.4 21.1, 47.3	31.6 ± 7.05 24.0, 39.7	27.9 ± 15.5 13.5, 54.0
Monoterpene SOC (μgC m^{-3})	40.1 ± 33.3 7.18, 154	62.7 ± 56.5 19.2, 154	40.7 ± 20.0 11.8, 57.7	19.3 ± 5.61 14.0, 25.2	35.5 ± 23.5 7.18, 62.7
Monoterpene SOC to OC (%)	2.0 ± 1.47 0.37, 5.74	3.65 ± 1.58 2.44, 5.74	2.15 ± 1.45 0.48, 3.88	0.87 ± 0.58 0.37, 1.48	1.58 ± 0.84 0.54, 3.13
Monoterpene SOC to total SOC (%)	64.5 ± 15.5 28.9, 86.5	53.4 ± 20.3 28.9, 74.0	61.9 ± 10.4 52.7, 78.9	68.4 ± 7.05 60.3, 76.1	72.1 ± 15.5 46.0, 86.5

[e]P: *cis*-pinonic acid + pinic acid

Table 3. Comparisons of the concentration (ng m^{-3}) of anhydrosugars, sugar and sugar alcohols in Gosan aerosols with those from different sites around the world.

Sampling sites	Anhydrosugars	Primary sugars	Sugar alcohols	References
Gosan, South Korea	**21.4**	**48.4**	**9.53**	**This study**
Chennai, India	131	12.5	6.13	Fu et al., 2010b
Mt. Tai, China (June)	224	61.1	125	Fu et al., 2012b
Alert, Canada	0.17	0.49	0.30	Fu et al., 2009a
Okinawa, western North Pacific	3.53	62.0	29.5	Zhu et al., 2015a, b
Chichijima, western North Pacific	1.13	23.3	23.4	Verma et al., 2015, 2018
Mt. Hua, China (Non-dust strom)	57.8	92.5	22.4	Wang et al., 2012
Mt. Hua, China (Dust strom)	44.5	162	25.7	Wang et al., 2012
Nanjing, China	209 (Lev)	12.7	50.8	Wang and Kawamura, 2005
Beijing, China	117	24.7	11.8	Kang et al., 2018a
Belgrade, Serbia	425 (Lev)	116	98.4	Zangrando et al., 2016
Maine, USA	13.9	28	8.31	Medeiros et al., 2006
Crete, Greece	14.4	32.3	6.53	Theodosi et al., 2018

1068

1069

1070

1071

1072

1073

1074

1075